

LIVERPOOL UNIVERSITY

MASTER OF RESEARCH

DECISION MAKING UNDER RISK AND UNCERTAINTY

**Robust Probabilistic Risk/Safety Analysis
of Complex Systems and Critical
Infrastructures**

Supervisors:

Author:

Roberto ROCCHETTA

Dr. Edoardo PATELLI

Dr. Matteo BROGGI

Dr. Sven SCHEWE

September 21, 2015

Summary

This report summarizes the research outputs carried out within the MRes in Decision Making under Risk and Uncertainty. The supervisors Edoardo Patelli, Matteo Broggi and Sven Schewe, involved in the project “Robust Probabilistic Risk/Safety Analysis of Complex Systems and Critical Infrastructures”, have considered of primary interest for the year to improve my knowledge on advanced methodologies for risk analysis and uncertainty quantification. Hence, classical uncertainty quantification approaches, generalized uncertainty quantification methodologies and new applications for health management of mechanical systems have been explored. It has been assumed that, in addition to a methodological review, best learning approach to be endorsed was a pragmatic one. Thus, real case studies and real applications have been analysed, more specifically three practical applications have been faced so far.

First, a purely classical uncertainty quantification problem have been tackled, named the “Uncertainties in GPS positioning” challenge. It is an academic challenge launched by French Institute for Transportation Science and Technology Geolocalisation Team (IFSTTAR/ CoSys/ Geoloc), jointly with the French Federation of Mathematical Games. The challenge have been accepted and faced in collaboration with three students of the risk institute. Although authors and supervisors have not considered the completed work novel enough to be published, it has been extremely beneficial for the MRes, especially thanks to the issues and problems tackled during the study. The main challenges were to deal with imprecise real world data, minimize computational time and combine classical uncertainty quantification techniques such as Monte Carlo to algorithms for optimization. It is worth remark that this unpublished work has been rewarded by the organizing groups and the Liverpool team won the second price in the international competition (first price between the groups). The interested reader is remanded to the web link for further details:

http://scmsa.eu/archives/SCM_FFJM_Competitive_Game_2014_2015_comments.pdf

The second case study consist of a challenge launched by the independent, not-for-profit membership association “National Agency for Finite Element Methods and Standards” (NAFEMS). This application has been retained good starting point to approach novel uncertainty quantifi-

cation methodologies, important tools to better cope with lack of information, imprecision and not consistent data. The challenge has been faced by adopting classical but also generalized (non-classical) uncertainty quantification approaches, therefore developing a more complex framework. The computational framework can be seen as the original contribution of the work, it allows to qualify uncertainty of the information regarding the model parameters, i.e. multiple intervals, sampled values, imprecise intervals. The numerical implementation and solution to the challenge have been summarised into a conference paper, recently presented during the last NAFEMS World Congress (2015), which took place in San Diego, USA over four days in June. The presenter M. Broggi has been awarded with the best presenter award. For the future, possible journal targets have been already identified. Two possible targets are “Advances in Engineering Software” and “Computer Methods in Applied Mechanics and Engineering” which are good quality journals treating computer science and engineering related problems. Indeed the work is relevant for the future research project, which are going to be focused on novel approaches for robust risk analysis of complex systems, therefore it will likely deal with robust quantification of the uncertainty arising due to randomness and imprecision in the data.

The third application tackled within the Master of research year is a Bayesian model updating used to assess and manage the health state of a mechanical component, a suspension arm. The main aims were to obtain an improved real-time crack detection framework accounting for different sources of uncertainty i.e. unknown crack parameters, randomness in the device parameters and noisy measurements. The advancement of the work has been recently summarized in a conference paper presented to the 25th edition of the conference, ESREL 2015, in Zurich. Also in this case, uncertainty quantification is an important part of the work and Bayesian updating framework have been tested under different perspectives. More specifically, in order to meet computational time requirements which are strong constraints for real-time applications, two surrogate model have been tested and selected. Furthermore, as known that effectiveness of the procedure demand for accurate likelihood definition, three different ad-hoc likelihood function have been applied and results compared and discussed. The framework resulted to be a useful tool which require further analysis and tests. Journal publication has been considered, possible targets are journals focused on prognostic health management and advanced Bayesian model updating frameworks.

Highlights

This section are summed up in bullet points the main contributions and achievements of two of the work proposed in the MRes academic year.

The NAFENS Challenge Problem

- Numerical rigorous framework to deal with incomplete, imprecise information.
- No unjustified hypothesis on data, no subjective and biased exemptions.
- Neglecting epistemic uncertainties might lead to severe over/under estimation of the reliability.
- Solution to the NAFEMS uncertainty quantification challenge problem shows effectiveness of the framework.

The Bayesian Updating Framework for Real-Time Crack identification

- Bayesian Model Updating to estimate posterior distribution of crack parameters.
- Three empirical likelihood investigated and two surrogate model have been investigated and discussed.
- Code parallelization strategy adopted and time saving framework thanks to surrogate model obtained.
- Aleatory uncertainty in the Young's modulus and measurement noises shows to be important factor in a good crack parameters updating.

Preliminary Conclusions and Future Directions

Risk is the potential of experiencing a loss when a system does not operate as expected due to the occurrence of uncertain and difficult-to-predict events. The more general qualitative definition of risk accounts for both uncertainty in the occurrence of hazardous events and the consequences of these events. Hence, it seems intuitively correct to consider the risk concept as pervasive and multidisciplinary by definition. In fact, discipline and sector of interest are involved depending on the type of consequences addressed and on the events considered in the study. Depending on the discipline, the Decision-Makers will have to face different risky decisions, all affected by uncertainties in at least one of its forms. Pointing out the limitations of uncertainty quantification approaches and improving the robustness of the decisions is hence essential to better understand what can change and what can go wrong in achieving goals. In order to increase the robustness of risk assessment several approaches and uncertainty quantification techniques have been reviewed during the year. Indeed classical uncertainty analysis is an important tool to obtain a representation of model predictions consistent with the state-of-knowledge and available information. Within an imprecise-information scenario, combination of probabilistic and non-probabilistic approaches are appealing tools to give different perspectives to the results without a demand of strong initial assumptions. The applicability of the different uncertainty quantification techniques has been confirmed useful by the NAFEMS challenge case study and the Bayesian Model Updating case study. The flexibility of the frameworks adopted in both the works will be further improved and tested on different real-life problems.

For the future are expected beneficial collaborations with the project partners, firstly with the industrial European Center for Soft Computing (ECSC) but also the academic partner professor Enrico Zio (Politecnico di Milano and/or Ecole Centrale de Paris). As an example, the ECSC research activity mainly focuses on research units such as fuzzy evolutionary applications, intelligent data analysis (data mining, pattern recognition), cognitive computing (computational systems able to provide linguistic descriptions of complex phenomena). Indeed their expertise in advanced risk analysis techniques and competence in dealing with uncertainty and imprecision are going to be the most important contribution to the final research output quality.

A Computational Framework for Classical and Generalized Uncertainty Quantification: Solution to the NAFEMS Challenge Problem

R. Rocchetta & M. Broggi & E. Patelli

Institute of Risk and Uncertainty, University of Liverpool, United Kingdom Tel.: 0044 (0) 151 7944079

ABSTRACT: Classical probabilistic approaches are well-established techniques often used to enhance robustness of simulations by accounting for uncertainty from different sources. Application of classical probabilistic frameworks, especially in cases affected by lack of information, may require strong initial assumptions often hardly justifiable. The assumptions made to deal with uncertainty due to data unavailability can deeply influence the final results and lead to severe risk misjudgement. Generalised probabilistic approaches have been recently introduced to better deal with scarce or limited information. The strengths and the shortcoming of classic and generalised approaches have been pointed out in literature. However, to help acceptance and to better understand their strengths, further comparisons seems to be needed, especially from an applicative prospective. In this paper, different probabilistic approaches are implemented in a common computational framework, which has been adopted to solve the NAFEMS uncertainty quantification challenge problem. Strength and weakness of both the methodologies have been directly faced and presented. The results obtained have confirmed that classic probabilistic approaches when bearing strong artificial assumptions may lead to misleading conclusion which not fully representative the real available information quality. Generalised probabilistic approaches have shown to be versatile and powerful tools.

1 INTRODUCTION

Nowadays, it is generally well understood that is necessary to include uncertainties in simulations, e.g. due to variation in parameters and operational conditions, in order to achieve robust design of new products, execute model validation or ensure reliable operation for the whole product-life. It is important that easy to follow and accurate guidance, best practices and computational tools are available to make uncertainty quantification a standard techniques adopted by a larger public of engineering practitioners.

Classical probabilistic approaches are well established techniques which can be used to enhance robustness of the desired results, accounting for uncertainties which can arise from different sources. However, in order to create probabilistic classical frameworks and overcome lack of or imprecise information, strong initial assumption may be needed and are often hardly justifiable. Those assumptions, such as predefined probability distributions, can substantially influence the final outcomes and especially in reliability analysis may led to misleading results (Beer, Ferson, & Kreinovich 2013).

Generalized approaches are powerful methodolo-

gies which could in some cases be coupled to the traditional approaches in order to give a different prospective on the results, enhancing the overall robustness. Examples of such flexible frameworks are provided by e.g. (Ferson, Kreinovich, Ginzburg, Myers, & Sentz 2002) and (Patelli, Alvarez, Broggi, & de Angelis 2014). In the last years some efforts have been putted in comparing different generalized and classical approaches, e.g. see (Zio & Pedroni 2013), (Laura P. Swiler 2009), (Alex Diaz De La O 2014). However, further confrontations of different methodology, especially applied to real study cases, are required to showcase and promote generalized approaches, as well as the use of dedicated software tools to automate the analysis.

In this paper, a computational tool useful to implement generalized and classical uncertainty quantification in a common framework is presented. The computational framework has been tested providing solution of the uncertainty quantification challenge problem proposed by the NAFEMS stochastic group (NAFEMS 2013). The problem is tackled by adopting classical, but also generalised probabilistic approaches, which fits in the framework of imprecise probabilities. The results obtained by these novel approaches, which account for both epis-

temic and aleatory source of uncertainty and require weaker initial assumptions, will be compared with the previous solution to take sides of the limitations and shortcomings of both the methodologies. This will confirm the increased flexibility in the uncertainty treatment found when also imprecise probabilities are employed, as well will provide guidance to implement classical and generalized approaches when different type of imprecise information is provided. Increased flexibility can be achieved by improving the uncertainty models with provided information of different quality and by efficiently including evidence from wide range of sources.

At the last NAFEMS world congress, held in 2013 Salzburg, the NAFEMS Stochastic Working Group has launched a challenge problem open to contributors from Academia, Government and Industry. The system subject to the analysis is a simple RLC series electric circuit with different levels of uncertainty estimated around the model input parameters (i.e., intervals from multiple sources, finite number of sampled values, incomplete intervals). The scope of the challenge was to evaluate the reliability of this circuit under the different input uncertainties as well as to quantify the value of information in each case. The interested readers are reminded to reference (NAFEMS 2013) and (NAFEMS 2014) for further details about the problem definition. This case study has been retained particularly suitable to be solved using probabilistic and also generalized approaches and serve as platform for further comparisons between different methodologies. The proposed computational framework has been embedded to OpenCOSSAN, see (Patelli, Broggi, Angelis, & Beer 2014), open general purpose software for uncertainty quantification which has been employed in all the steps of the analysis.

This paper is structured as follows: Section 2 presents theoretical background, a brief review of generalized approaches and an introduction to Dempster-Shafer methodology. In Section 3 a synthetic overview the numerical framework is made. Section 4 shows the NAFEMS challenge problem, the reliability requirements and computational challenges. In Section 5 the classical and generalized approaches and results for the different tasks of the challenge are presented. In Section 6 a brief discussion on the limitations of the different approaches is presented In Section 7 conclusions are drawn.

2 THEORETICAL BACKGROUND

Uncertainties can generally be described in two groups, the so called aleatory and epistemic uncertainties (Der Kiureghian and Ditlevsen 2009). The aleatory, also indicated in literature as Type I or irreducible uncertainty, is related to stochastic behaviours

and randomness in events and variables. Hence, due to its intrinsic random nature is normally regarded as not reducible, that means the degree of uncertainty cannot be decreased even if the knowledge of the system or of the physical phenomena is improved. The epistemic, also called Type II or reducible uncertainty, is commonly related to lack of knowledge about a particular behaviour, imprecision in measurement and poorly designed models. It is considered as reducible since further data can reduce the level of uncertainty, but this is not always practical or feasible.

The Monte Carlo is a broadly applied classical approach often used to deal with uncertainties without differentiates between aleatory and epistemic types (Marseguerra and Zio 2002). It has been considered in the study because is flexible and is one of the most well-established classical methodology to characterize and propagate uncertainty. As mentioned, the Monte Carlo (MC) approach has been applied in several survey, e.g. Rocchetta et al. 2015 and Ching and Chen 2007, no further details about this technique will be provided in this paper.

Nevertheless, it is well-understood that MC approach have to face serious limitation, especially in the computational aspect, e.g. high number of simulations are needed in order to sample just one rare event. Moreover, MC classical approach cannot differentiates between aleatory and epistemic uncertainty, hence assumptions may be needed to deal with imprecise information. In the last decades, efforts were focused in the treatment of imprecise knowledge, non-consistent information and both epistemic and aleatory uncertainty by efficient approaches. The methodologies are discussed in literature by different mathematical concepts: Dempster-Shafer Evidence theory (Dubois and Prade 1988, Shafer 1976, interval probabilities (Augustin 2004), level two probably approach (Helton et al. 2004, Pedroni et al. 2013), Fuzzy-based approaches (Blair et al. 2001) and Bayesian updating approaches (Faber 2005 Kiureghian 2008, Veneziano et al. 2009 Ching and Chen 2007), are some of the most intensively applied concepts.

Considering all the reviewed methodologies, the Dempster-Shafer approach based on the theory of Evidence has been selected to tackle the challenge problem through a generalized framework. The main reasons for this selection are that Dempster-Shafer approach requires little assumption and can be easily implemented and coupled to classical probabilistic frameworks; moreover it is generally applicable allowing solving all the tasks proposed in the challenge problem. Kolmogorov-Smirnov test and Kernel Density Estimator have been also used to represent the sample uncertainty for extremely small sample size, one of the challenge tasks (see Section 4) The

first is used combined to Dempster-Shafer approach in a Generalized framework; the latter is combined to Monte Carlo simulation to provide a classical solution to the task.

2.1 Dempster-Shafer Structures and Probability Boxes

One of the largely used frameworks of subjective probability is the Dempster-Shafer theory which is a well-suited framework to represent both aleatory and epistemic uncertainty and it can be seen as a generalization of Bayesian probability. In the Dempster-Shafer theory, numerical measures of uncertainty (a degree of belief also referred to as a mass) may be assigned to overlapping sets and subsets of hypothesis, events or propositions as well as individual hypothesis, see e.g. Beer et al. 2013. Probability values are assigned to sets of possibilities rather than single events. In the Shafer theory the sets are represented as intervals, bounded by two values, belief and plausibility.

In order to characterize both epistemic and aleatory uncertainty, probability boxes (referred as P-boxes) are often used. P-boxes can be seen as a further generalization of the Dempster-Shafer structures where the sets are represented by distributions. The Dempster-Shafer structures are similar to discrete distribution but rather than precise points, the locations where the probability mass resides are set of real values, it can be expressed as set of focal elements as presented by Ferson et al. 2002:

$$(([\underline{x}_1, \bar{x}_1], m_1), ([\underline{x}_2, \bar{x}_2], m_2), \dots, ([\underline{x}_n, \bar{x}_n], m_n)) \quad (1)$$

Where $[\underline{x}_i, \bar{x}_i]$ is the i^{th} focal element with upper bound \bar{x}_i and lower bound \underline{x}_i , m_i is the probability mass associated with the i^{th} focal element. P-boxes are set of cumulative distribution functions (CDFs) for which lower and upper bounds are assigned $[\underline{F}_X, \overline{F}_X]$. Note that the probability distribution associated to the random variable of interest can be either defined or not. As summarized by (Patelli et al. 2014) the first are generally named distributional P-boxes (or parametric P-boxes) the latter are called distribution-free P-Boxes (or non-parametric P-Boxes). Figure 1 shows an illustrative example of distributional P-Box, the parent distribution is the normal distribution; the red dashed line is the lower bound \underline{F}_X , black solid line is the upper bound \overline{F}_X .

The wider the distance between upper and lower bound the higher epistemic uncertainty is associated to the random variable. The bounds for the CDFs mean bounds on probabilities, upper and lower probability bounds can be hence obtained as:

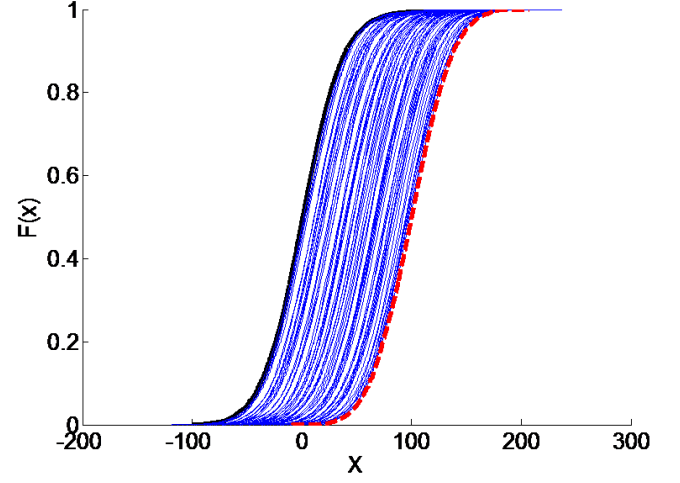


Figure 1: Illustrative example of distributional P-Box.

$$\overline{F}_X = \overline{P}(X \leq x) = 1 - \underline{P}(X \leq x) \quad (2)$$

$$\underline{F}_X = \underline{P}(X \leq x) \quad (3)$$

In literature the lower bound on probability is sometime referred as plausibility Equation (4) (and the upper bound as belief, Equation (5)). Cumulative Plausibility and Belief function can be computed as:

$$Pl(z) = \sum_{x_i \leq z} m_i \quad (4)$$

$$Bel(z) = \sum_{y_i \leq z} m_i \quad (5)$$

Dempster-Shafer structures can be always translated into a P-box but without forgetting that is not an information preserving procedure. These approaches are straightforward to deal with some of the cases proposed in the NAFEMS challenge, such as multiple and overlapping intervals and inconsistent sources of information. The drawback is that the propagation of intervals and P-boxes through the system can results computational expansive. Nevertheless, the quantification approaches are generally not-intrusive and hence applicably to any model. For further acknowledgement the reader is reminded to Laura P. Swiler 2009. This is an interesting feature of the approach which is therefore suitable to be used in parallel to classical uncertainty quantification method to give wider prospective on the analysis.

2.2 The Kernel Density estimator

It is in general difficult to get the true distribution from a small number of samples using parametric methods. This is because there is no enough information to estimate the PDF when only few data points are available. Kernel density estimator is another non-parametric approach that can be used to estimate the probability density function of a random variable

(Pradlwarter and Schuller 2008). The approach does not need any assumptions regarding the underlying distribution. A commonly used univariate parametric kernel is the Gaussian or normal Kernel:

$$\hat{f}(x) = \frac{1}{n\sigma\sqrt{2\pi}} \sum_{i=1}^n \left(\frac{-(x-x_i)^2}{2\sigma^2} \right) \quad (6)$$

where $\hat{f}(x)$ represents the estimated probability density function of n samples x_i drawn from an unknown density function f . The variance (or bandwidth) σ^2 is the only parameter that needs to be estimated. The best bandwidth can be estimated using for instance the Silverman's rule of thumb (Silverman 1986) or in case of very small sample sizes the approach proposed by Pradlwarter and Schuller 2008.

2.3 Kolmogorov-Smirnov Test

The so called Kolmogorov-Smirnov statistical test (Massey 1951) is one possible non-parametric approach that can be used to characterize the uncertainty of a process starting from samples with a reference probability distribution. The Kolmogorov-Smirnov (KS) test is a distribution-free statistical test based on the maximum difference between an empirical CDF and a hypothetical CDF. It returns upper and lower bound of CDFs assuming a predefined confidence level. The bounds can be computed by use of Equation (7) as:

$$\min(1, \max(0, DF(x), D(\alpha, n))) \quad (7)$$

where $DF(x)$ denotes the best estimate of the distribution function and $D(\alpha, n)$ is the one-sample KS critical statistic for confidence level $100(1 - \alpha)\%$ where α is the selected significance level and n the sample size. The KS critical statistic can be therefore used to obtain different confidence limits on the CDFs by choosing different critical values of the statistic test. Different level of confidence lead to different confidence bounds on the CDFs which, when propagated, produce boarder or narrow bounds of the resulting P-boxes.

3 NUMERICAL IMPLEMENTATION

Generalized and classical probabilistic uncertainty quantification methods are powerful techniques to deal with uncertainty and combine methodologies in a common computational framework is of high interest for the uncertainty analyst. OpenCossan is a collection of methods and tools under continuous development, coded exploiting the object-oriented Matlab programming environment. It allows defining specialized solution sequences including any reliability

methods. Hence optimization algorithm, new reliability methods or uncertainty quantification and propagation techniques can be easily added. In the presented work a computational tool useful to implement Generalized and Classical probabilistic approaches in a common framework is presented. Schematic representation of the computational framework is shown in Figure 2.

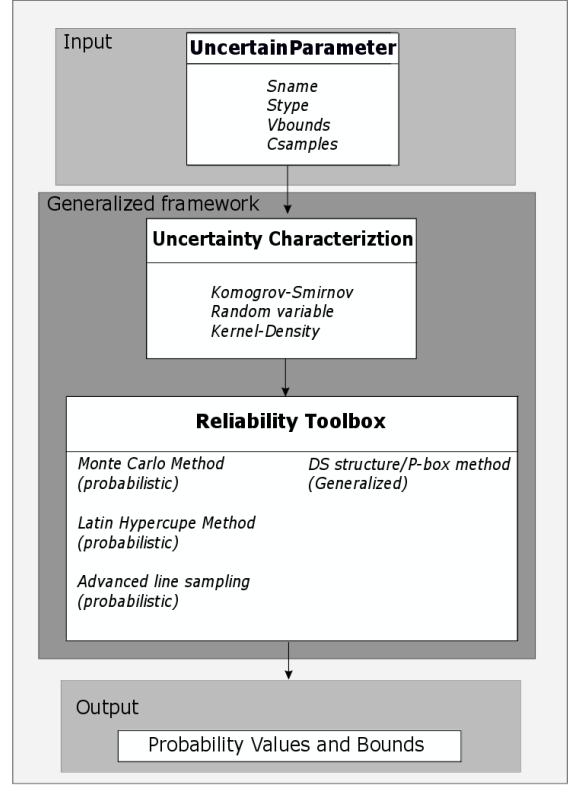


Figure 2: Simplified representation of the computational tool

Algorithm 1 Dempster-Shafer structures Propagation Algorithm

```

1: procedure DS PROPAGATION
2:   for each Parameter j do
3:     Assign mass  $m_i^j \forall$  focal elements  $i \in$  Parameter j
4:   end for
5:   if  $\sum_i m_i^j \neq 1$  then
6:     ERROR. Masses have to be normalized
7:   end if
8:   for each  $\omega \in \Omega$  which is the set of all possible interval combinations do
9:     for  $K=1$ : last performance variable do
10:      Compute Minimum and Maximum of  $K$ 
11:       $[Min(K), Max(K)]_\omega$ 
12:    end for
13:    Compute mass for the combination  $\omega$ 
14:     $m_\omega = \prod_j m_i^j$ 
15:    Save  $[Min(K), Max(K), m]_\omega$ 
16:  end for
17:  Save the Propagated DS structure
18:   $([Min(K), Max(K), m]_1, \dots, [Min(K), Max(K), m]_\Omega)$ 
19:   $\forall$  variable  $K$ 
20: end procedure

```

In the proposed framework, the parameters information is stored in *UncertainParameter* which contain parameters name, type of uncertainty and numerical information such as bound values or samples values. The propriety *Stype* identify the uncertainty type affecting the parameter e.g. single or multiple intervals, samples or imprecise intervals for which only upper or lower bound are well defined. Whereupon *UncertainParameter* is defined, parameter uncertainty is further characterized by use of Kolmogrov-Smirnov test, Kernel Density estimation or by defining random variables from a set of well-known distribution (e.g. uniform). Depending on the uncertainty type, only some characterization and propagation methodology are available, as schematically explained in Table 1. Among the different reliability and uncertainty propagation methods not just classical methods are available, e.g. Monte Carlo, Latin Hypercube, but also some generalized methods such as Dempster-Shafer (DS) propagation and P-box approaches.

Table 1: Scheme of Methods for the uncertainty characterization propagation depending on the uncertainty type

Type of uncertainty	Characterize	Propagate
Single or Multiple Intervals	Random Variable, DS structure	Monte Carlo, DS propagation
Sampled Values	Kernel Density, Kolmogrov Smirnov test	Monte Carlo, P-box propagation
Imprecise Intervals	Random Variable, DS structure	Monte Carlo, Line Sampling, DS propagation

Pseudo-code for the Dempster-Shafer structure propagation is presented in Algorithm 1. Further details on the propagation algorithm are provided in section 5.1.

4 THE NAFEMS CHALLENGE PROBLEM

The challenge problem, prepared by the stochastic group NAFEMS (2013), consist of four uncertainty quantification and information qualification tasks, ideate to identify and promote to the industry best practices to deal with uncertainty. In the challenge, the analysts are asked to evaluate the reliability of an electronic resistive, inductive, capacitive (RLC) series circuit shown in Figure 3, on meet performance requirements.

Four different cases (A, B, C and D) have been proposed, each one having incomplete, scarce or imprecise information about the system parameters, as

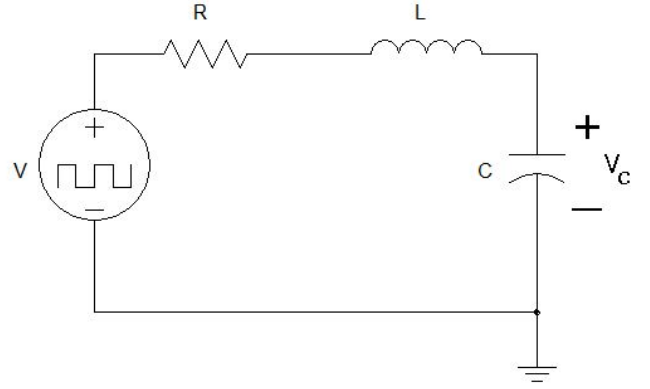


Figure 3: RLC series circuit. Input signal is the step voltage source for a short duration. Output response is the voltage at the capacitor.

Table 2: CASE-A CASE-B CASE-C and CASE-D, available information

CASE A	R[Ω]	L[mH]	C[μF]
Interval	[40,1000]	[1,10]	[1,10]
CASE B	R[Ω]	L[mH]	C[μF]
source 1	[40,1000]	[1,10]	[1,10]
source 2	[600,1200]	[10,100]	[1,10]
source 3	[10,1500]	[4,8]	[0.5,4]
CASE-C	R[Ω]	L[mH]	C[μF]
Sampled Data	861, 87, 430, 798, 219, 152, 64, 361, 224, 61	4.1, 8.8, 4.0, 7.6, 0.7, 3.9, 7.1, 5.9, 8.2, 5.1	9.0, 5.2, 3.8, 4.9, 2.9, 8.3, 7.7, 5.8, 10, 0.7
CASE D	R[Ω]	L[mH]	C[μF]
Interval	[40, R_{U1}]	[1, L_{U1}]	[C_{L1} , 10]
Other info	$R_{U1} > 650$	$L_{U1} > 6$	$C_{L1} < 7$
Nominal Value	650	6	7

shown in Table 2. In the CASE-A single intervals, one upper bound and one lower bound for parameter R L and C are given. In the CASE-B, each parameter can lay within multiple intervals, i.e. three upper and lower bounds. In CASE-C small sample sizes of ten sampled points for each parameter are provided. Finally for the CASE-D, imprecise bounds are the only available information; this last case is similar to CASE-A, but one bound is not precisely defined. Uncertainty is characterized using different classical and generalized approaches according to the level of knowledge available for the parameters R, L and C.

The equations governing the RLC circuit are provided by the challengers. The transfer function of the system is defined as:

$$\frac{V_c(t)}{V} = \frac{\omega^2}{S^2 + \frac{R}{L}S + \omega^2} \quad (8)$$

Depending on the values of R, L and C, the system

may be classified as under-damped critically damped or over damped.

Under damped ($Z < 1$):

$$V_c(t) = V + (A_1 \cos(\omega t) + A_2 \sin(\omega t)) \exp^{-\alpha t} \quad (9)$$

Critically damped ($Z = 1$):

$$V_c(t) = V + (A_1 + A_2 t) \exp^{-\alpha t} \quad (10)$$

Over damped ($Z > 1$):

$$V_c(t) = V + (A_1 \exp^{S_1 t} + A_2 \exp^{S_2 t}) \quad (11)$$

where roots are computed as:

$$S_{1,2} = -\alpha \pm \sqrt{\alpha^2 - \omega^2} \quad (12)$$

and damping factor Z , values of ω and α are determined as follow:

$$\alpha = \frac{R}{2L}; \omega = \frac{1}{\sqrt{LC}}; Z = \frac{\alpha}{\omega} \quad (13)$$

Coefficients A_1 and A_2 are determine by assuming initial voltage and voltage derivative equal zero, unitary step voltage function were considered.

In the challenge, the main goals consist in qualify the value of information and evaluate the reliability of the system with respect to three requirements. The first two are on the voltage at the capacitance V_c (since the second requirement on rise time can be translated into a voltage requirement as well). More specifically:

$$V_c(t = 10ms) > 0.9V \quad (14)$$

$$V_c(t = t_r) > 0.9V \quad (15)$$

where t_r is the voltage rise time, the time from 0 to 90% of the input voltage, and have to be less than 8 ms. The third requirement is on the under-damped system responses which have to be discharged ($Z \leq 1$). It can be observed that the third requirement imply a monotonic behaviour for V_c , therefore it is trivial rewrite the second requirement as in Equation (16):

$$V_c(t = 8ms) > 0.9V \quad (16)$$

The cumulative distribution function (CDF) of a random variable is commonly used in reliability analysis to extract useful knowledge about the so called probability of failure as follows:

$$F_X(x) = P(X \leq x) \quad (17)$$

Specifically, $V_c(10ms)$, $V_c(8ms)$ and Z are considered as random variable and Equation (17) can be used to compute the probabilities that the system fail on meet the three requirements by estimating $F_{V_c(10ms)}(0.9)$, $F_{V_c(8ms)}(0.9)$, and $F_Z(1)$

If bounds on the CDFs are obtained, Equations (2)-(3) can be used to compute the bounds on probability of not meet the requirements, $[\underline{P_{V_c10fail}}, \overline{P_{V_c10fail}}]$, $[\underline{P_{trfail}}, \overline{P_{trfail}}]$, and $[\underline{P_{Zfail}}, \overline{P_{Zfail}}]$.

5 CLASSICAL AND GENERALIZED APPROACHES FOR THE NAFEMS CASES SOLUTION

Within this section, classical and generalized approaches are adopted to tackle the four cases of the NAFEMS challenge problem. Uncertainty characterization, propagation are presented for each case, furthermore available information quality and system reliability is discussed.

5.1 CASE A and CASE B

In CASE-A single interval information is provided for the parameters (see, Table 2) while multiple interval information is available in CASE-B. Adopting the generalised probabilistic method and in particular the Dempster-Shafer approach, the CASE-B degenerate to CASE-A if probability mass equal one is assigned to the first source of information. This because in CASE-B intervals values for source 1 correspond to interval values in CASE-A. Due to the considerations made, the two cases are presented and solved together.

Classical Approach

In the Case-A, a Monte Carlo simulation-based approach has been implemented. Classical probabilistic approaches do not allow to model explicitly intervals. A largely used approach is to model the parameters as random variables which may vary uniformly between the provided interval bounds, assumption made with respect to the Principe of maximum entropy. However, this implies that each value inside the interval is equally probable and this is a very strong assumption that might not be justified by the evidence from experimental data or expert judgement. Uncertainty propagation and reliability assessment are performed by randomly sample R L and C from the associated uniform distributions and evaluating if the system requirements are met (e.g. system is under failure with respect to the first requirements, if Equation (14) is not satisfied).

The solution of the Case-B follows the same procedure as the Case-A. Each interval is considered individually. Hence, three different uniform distributions for each R , L , and C variables are used to modelling, one for each source of information. The reliability analyses have been performed to estimate compute 3 probabilities of failure, one for each source of information. Furthermore, for comparative purpose, overall probability of failure is obtained in CASE-B by averaging the results, this is done assuming each source of information as equally likely.

Table 3: Results CASE-A, comparison between Coefficients of Variation when computing different samples.

CASE-A	1000 samples		10000 samples	
	Prob.	Cov	Prob.	Cov
$P_{V_{c10_{fail}}}$	0.284	0.050	0.268	0.017
$P_{tr_{fail}}$	0.346	0.044	0.364	0.013

Table 4: Results CASE-B: Monte Carlo resulting probability of failure for the three sources, 10000 samples.

CASE-B	Source 1	Source 2	Source 3	Mean Sources
$P_{V_{c10_{fail}}}$	0.270	0.512	0.123	0.303
$P_{tr_{fail}}$	0.354	0.670	0.209	0.411

Classical Results

The Monte Carlo simulation has been performed in order to compute failure probabilities and Covariance for CASE-A and CASE-B. First, the failure probabilities has been estimated using 1000 samples, secondly new analyses with 10000 samples has been carried to compare the Coefficients of Variation (Cov) of the estimated probabilities, as shown in Tables 3. It has been noticed that, as in the CASE-A, also in CASE-B the probability of failure slightly changes even after increasing the samples. The probability of fail to meet the requirement one, as expected, is lower than the probability of fail to meet the requirement two.

It is possible to see from Table 4 that the system considering source 2 has the lower reliability. In 1000 samples, approximately 512 will be out of the first requirements. The Source 3 has the lowest estimated probability of failure and the Source 1 shows an intermediate Probability of failure. The averaged probability of failure is about 0.3 and 0.41 for the first and second requirement, respectively.

Generalized Approach

The intervals that define the possible values of the parameters can be represented by means of the generalised probabilistic approach without making any assumption about the possible distribution of the values. Parameter uncertainty has been characterized by use of Dempster-Shafer structures. A general Dempster-Shafer structure for each parameter is defined by Equation (1). For CASE-A three Dempster-Shafer structures composed by a single focal element have been defined as follows:

$$([R_1, \bar{R}_1], m_1) ([L_1, \bar{L}_1], m_1) ([C_1, \bar{C}_1], m_1) \quad (18)$$

where m_1 is equal one. For CASE-B, three structures have been considered as in Equation (19)-(21), each composed by three focal elements:

$$([R_1, \bar{R}_1], m_1), ([R_2, \bar{R}_2], m_2), ([R_3, \bar{R}_3], m_n) \quad (19)$$

$$([L_1, \bar{L}_1], m_1), ([L_2, \bar{L}_2], m_2), ([L_3, \bar{L}_3], m_n) \quad (20)$$

$$([C_1, \bar{C}_1], m_1), ([C_2, \bar{C}_2], m_2), ([C_3, \bar{C}_3], m_n) \quad (21)$$

$$m_1 + m_2 + m_3 = 1 \quad (22)$$

where $[R_i, \bar{R}_i]$ represents the i^{th} interval bound for the resistance, $[L_i, \bar{L}_i]$ is the i^{th} bound for the inductance, $[C_i, \bar{C}_i]$ is the i^{th} bound for the capacitance and m_i is the probability mass associated to the i^{th} source. The probability masses associated to the different sources have been considered equal and normalized. The CASE-B degenerate to the CASE-A if the probability mass m_2 and m_3 are set equal to zero. It is not possible here to establish if some sources of information are better, thus information derived from different sources is assumed as equally likely.

Dempster-Shafer structures Propagation

The following procedure was adopted in order to propagate the uncertainty characterized by Dempster-Shafer structures:

- First, probability mass is assigned to each focal element (interval) of R L or C, e.g. for CASE-B m_1, m_2, m_3 are assigned to intervals of source 1 2 and 3, respectively.
- n 'Parameter cells' are constructed by permutation of the focal elements, i.e. in CASE-B $n=3!$. The first parameter cell is built by selecting the first interval of the parameter R and first interval of the parameter L and combining them with the first interval of C. The second cell is built selecting the first interval of R and first of L and combining them with the second interval of C, so on in a combinatorial manner .
- For each cell, Latin Hypercube Sampling (LHS) strategy is used to samples parameter values. Then the system responses are evaluated in terms of V_c and Z and the minimum and maximum of the outputs are calculated. An alternative approach based on optimization technique can be used to identify the output bounds for interval cells .
- The results are stored and n min-max intervals of $V_c(8ms)$, $V_c(10ms)$ and n min-max interval of Z are saved, each interval correspond to a focal element for the output of interest. The Results are used to create Dempster-Shafer structures, see Equation (1), where probability masses have been assigned depending on the probability masses of the focal elements composing the cells. As example Dempster-Shafer structure for Z and $V_c(8ms)$ will result:

$$([Z_1, \bar{Z}_1], m_{c1}), \dots, ([Z_n, \bar{Z}_n], m_{cn})$$

$$([V_c(8)_1, \bar{V}_c(8)_1], m_{c1}), \dots, ([V_c(8)_n, \bar{V}_c(8)_n], m_{cn})$$

Where the probability mass computed for n parameters cells are $m_{c1} = m_1 m_1 m_1$, $m_{c2} = m_1 m_1 m_2$, etc.

- Finally intervals the Dempster-Shafer structures are used ,as explained in (Ferson et al. 2002), to create probability boxes of $V_c(8ms)$, $V_c(10ms)$ and Z . Equations (4)-(5) are used to compute the Belief and Plausibility bounds and failure probability intervals.

Generalized Results

Applying the procedure to the CASE-A, the resulting P-boxes gave no valuable information on the failure probability for the three performance requirements. The probability of failure is in fact just bounded in the interval $[0,1]$ for all three the requirements.

In CASE-B equal probability mass have been assigned to the three distinct sources of information, such that $m_1 = m_2 = m_3 = 1/3$. The resulting P-boxes of V_c and Z are shown in Figures 4-6. Resulting bounds are presented in Table 5, it can be seen that outputs have high uncertainty associated, but reduced if compared to the Case-A. Figure 5 shows that $P_{tr_{fail}}$ lay within the interval $[0,0.9]$. It can be also observed that $P_{Z_{fail}}$ upper and lower bounds are $[0,0.7]$ and that $P_{V_{c10}_{fail}}$ lay within the interval $[0,1]$. The CASE-B includes all the information available for the CASE-A (information in source 1 coincide with information of CASE-A) plus two additional sources of information. In this particular case, the additional sources of information contribute on reducing the uncertainty on the system performance.

Comparison between CASE-B and A show that the first produces narrower intervals for the probability of fail to meet requirement one and three. On the other hand, failure probability for requirement two do not show any uncertainty. It can be therefore argued that, with respect to the first and third requirements, the quality of the information given in CASE-B is higher compared to the quality of the information given in CASE-A. On the other hand, results have the same quality with respect to the second reliability requirement.

By comparing classical and generalized results, values obtained for the failure probability (classical approach) lay within the bounds obtained using the Dempster-Shafer methodology (generalized approach). Obtaining a solution for the generalized approach point out that the uncertainty affecting the information for both CASE-A and CASE-B seems to be strongly underestimated by the classical approach. This is probably due to the assumption made on the parent distribution needed to apply classical methodology.

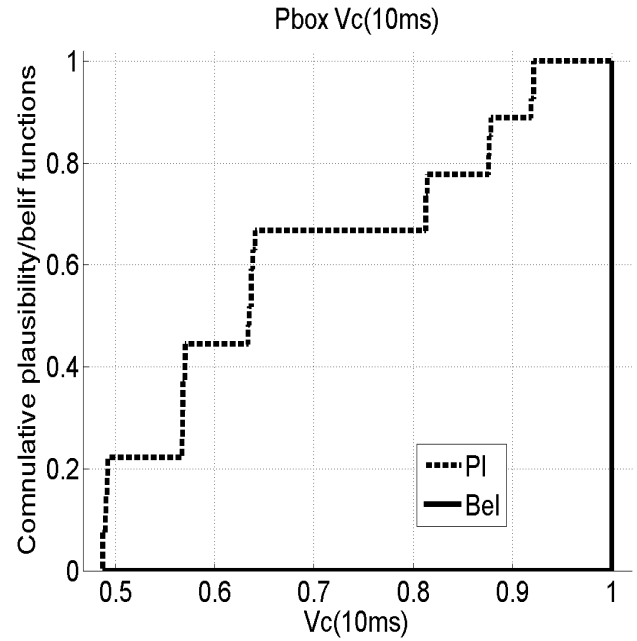


Figure 4: P-box $V_c(10ms)$ CASE-B

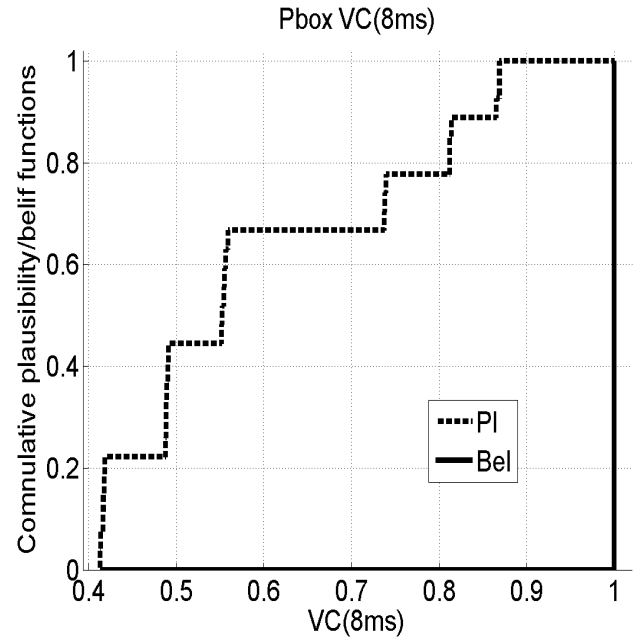


Figure 5: P-box $V_c(8ms)$ CASE-B

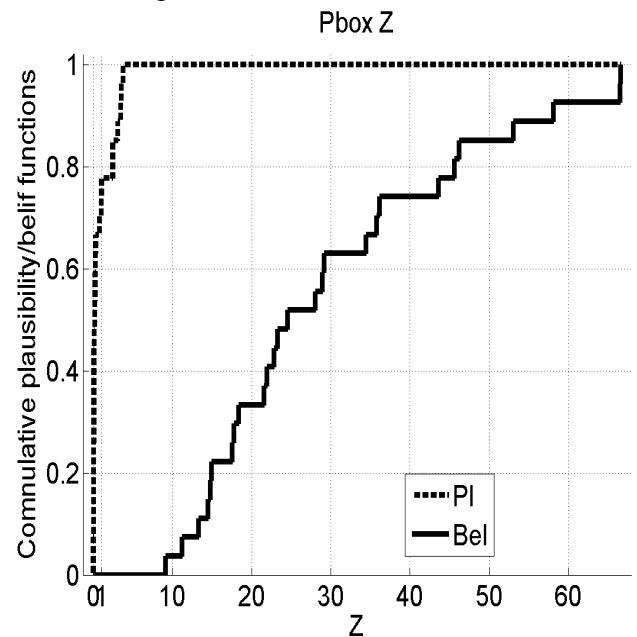


Figure 6: P-box Damping coefficient CASE-B

Table 5: Results CASE-B, comparative table.

CASE-B	Source 1	Source 2	Source 3	All Sources
$P_{V_{c10_{fail}}}$	[0,1]	[0,1]	[0,1]	[0,0.9]
$P_{tr_{fail}}$	[0,1]	[0,1]	[0,1]	[0,1]
$P_{Z_{fail}}$	[0,1]	[0,1]	[0,1]	[0,7]

5.2 CASE C

The available data consists of 10 sampled values for each parameter of R, L and C, respectively. Table 3 summarize the parameter information given for CASE-C. No additional information about the parameter such as, sampling procedure or parent probability distribution functions has been provided.

Classical Approach

Two classical approaches for the solution CASE-C have been developed:

First, only finite number of combinations of the input values is accounted. A Full Factorial Design of Experiments (DOE) was created to generate all the possible combinations of the defined points and a failure analysis was performed for each of them. This approach is fast and rather easy to implement, but clearly have severe limitations, e.g. assume that sampled values are the only allowed values for the parameters.

In the second classical approach, the Kernel Density Estimator (KDE) is used to fit probability distribution to small sample data. Probability distribution functions for the parameter have been fitted using the small samples and the Gaussian Kernel Density estimation as explained in subsection 2.2. Then, a Monte Carlo simulation is carried out to sample parameters value from the fitted distributions, the system performance is evaluated and the reliability computed. This second approach has been implemented assuming a Gaussian Kernel and assuming samples as independent samples of a random variable.

Classical Results

First attempt to solve classically CASE-C consider only a finite number of parameter values and parameter combinations. Just 10 sampled points for each element R, L and C are available, which means 1000 possible combinations. Within the 1000 possible combinations, 150 lead to system requirement failure because $V_c(10ms)$ was lower than 0,9V, 230 input combinations produce rise times greater than 8ms and 71 input combinations lead to under-damped responses. The Figure 7 shows combinations of input values that produce systems that satisfy or not each requirement. Note that the probabilities of failure are exact, not an estimation, since all the possible combinations were analysed. Red triangular marks correspond to failure

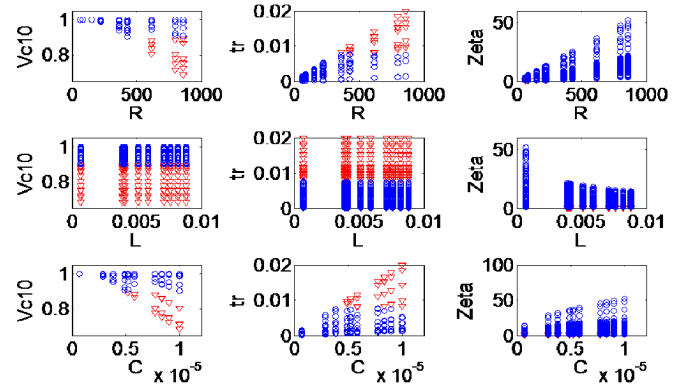


Figure 7: Design of experiment results

combinations, blue dots correspond systems which have sanctified the requirements.

In the second approach, the Kernel Density Estimator is used to fit probability distribution to small sample data. The results obtained in the first classical approach, which adopted Design of experiment to represent the uncertainty are $P_{V_{c10_{fail}}}=0.15$, $P_{tr_{fail}}=0.23$ and $P_{Z_{fail}}=0.071$. Kernel Density fitting and Monte Carlo sampling from the fitted distributions lead to probability slightly major if compared to the DOE solution, $P_{V_{c10_{fail}}}=0.232$, $P_{tr_{fail}}=0.292$, $P_{Z_{fail}}=0.121$. This is probably due to the longer tail of the parameters fitted by KDE, which result having a very long right tails. Figures 8-10 shows the resulting CDFs, Z CDF has been zoomed around the value $Z=1$ for graphical reasons.

Compared to the results obtained for CASE-A applying classical methodology, the probability of failure for CASE-C result generally lower. Same consideration can be done by comparison to the overall results obtained for case CASE-B but not all the single sources of information.

Generalized Approach

CASE-C has been solved also by using generalized approaches, first confidence bounds have been obtained by applying the KS test, see Section 2.3. After this first characterization for the sample uncertainty the obtained P-boxes for the parameter are propagated through the system and the outputs of interest computed. The uncertainty propagation procedure adopted is similar to the procedure used in CASE-A and CASE-B. Three different confidence levels are been considered for the KS test, therefore three different bounds have been propagated. To characterize the uncertainty, Kolmogorov-Smirnov critical statistic is used as shown in Equation (7). The results are bounds on the empirical distribution function of the sampled parameters. Figures 11-13 display upper and lower bounds (dashed and solid black lines) for the empirical CDF (solid blue line) of the inductance L, R and C. The bounds in figure refer to a confidence level $\alpha=0.05$. Some assumptions have to be made in order to apply the KS test, the samples are regarded as independent and identical distributed and maximum

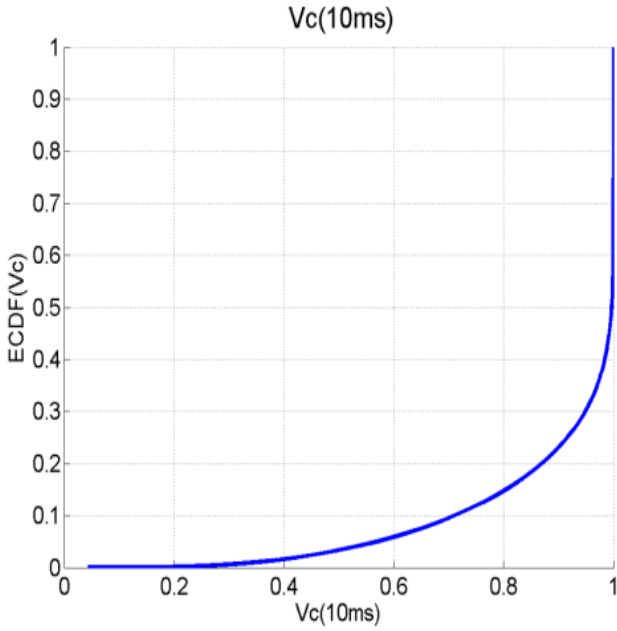


Figure 8: CDF of $V_c(10\text{ms})$ CASE-C

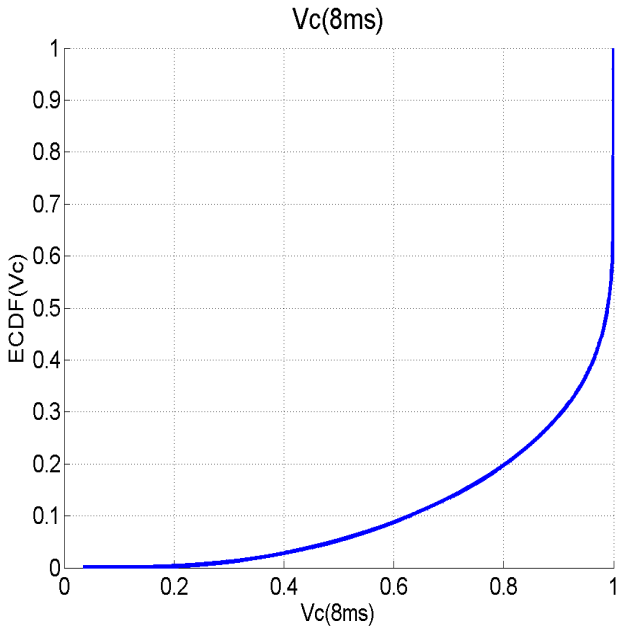


Figure 9: CDF of $V_c(8\text{ms})$ CASE-C

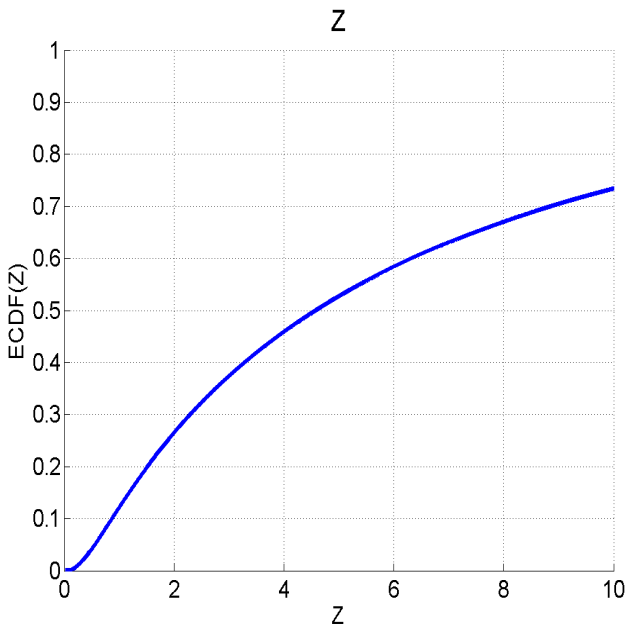


Figure 10: CDF of Z

Table 6: Results CASE-C, probability Bounds for the three requirements, three confidence levels .

CASE-C	$\alpha=0.01$	$\alpha=0.1$	$\alpha=0.2$
$P_{Vc10fail}$	[0,0.87]	[0,0.7]	[0,0.63]
P_{trfail}	[0,0.92]	[0,0.77]	[0,0.7]
P_{Zfail}	[0,0.83]	[0,0.7]	[0,0.64]

and minimum parameter values have been assumed in order to truncate the CDF bounds. Due to physical constraint, all the parameters must be positive and this condition allows to set then lower bound. The upper bound is in first instance assumed equal to the sample mean plus three times the standard deviation of the samples. It is important to notice that very long tails if underestimated can lead to safety overconfidence especially in reliability studies. Hence, following the considerations made, it has been selected a relatively high upper bound to truncate the CDF. In order to better investigate the goodness of the assumptions, analysis of the results (i.e. Failure probability) due to the variation of the assumed upper bounds has been performed. An increasing of the upper bounds (e.g. 6 time the standard deviation of the sample) slightly change the resulting probability bounds, as displayed in Figure 14.

Generalized Results

Even for CASE-C, the failure probabilities obtained by classical approach lay within the probability interval obtained by Generalized approaches. In Figures 15-17 P-Boxes for the voltage at the 10th ms, 8th ms and Z are presented, red blue and black colour lines refer to $\alpha=0.01$, $\alpha=0.1$ and $\alpha=0.2$ respectively. Figure 17 has been zoomed around the value $Z=1$ for improve the graphical output. Each confidence level lead to different probability bounds on the CDFs and resulting P-Boxes. The bounds on probability of fail to meet the requirements are shown in the Table 6. It can be noticed that, on the first hand probability intervals still wide, as already observed in CASE-A and CASE-B, which is typical of case denoted by high epistemic uncertainty. On the second hand, CASE-C shows an increased precision compared to the CASE-B and A. The resulting failure probability bounds obtained applying Dempster-Shafer approach to CASE-C, appear less uncertain compared to all the four cases. This increased precision may find intuitive explanations in the assumptions made in order to apply the Kolmogorov-Smirnov approach or may be due to the higher quality of the information provided in the challenge. Also for CASE-C, results show that uncertainty on the system reliability has been underestimated by using the classical approaches.

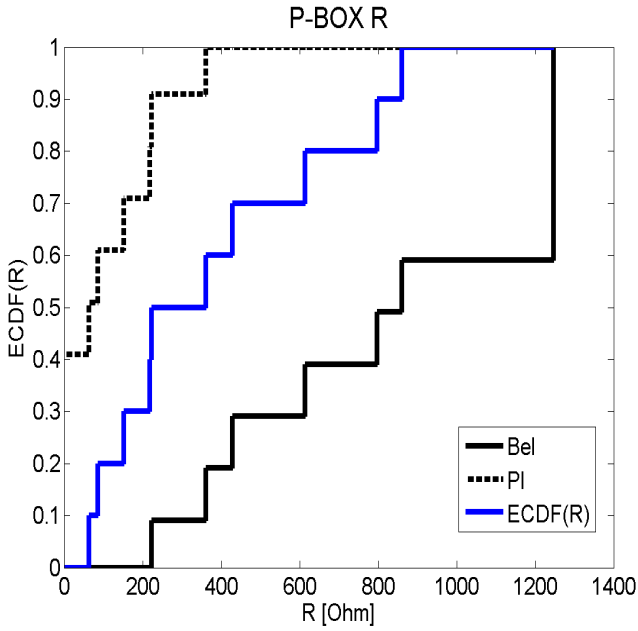


Figure 11: P-box R parameter CASE-C

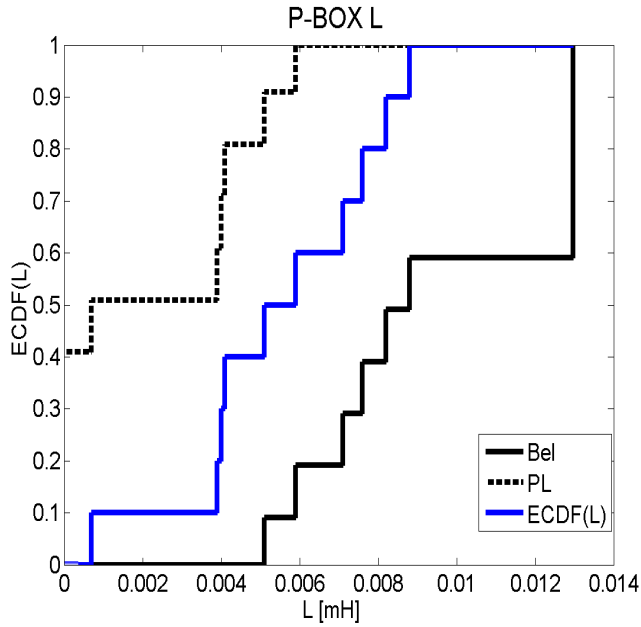


Figure 12: P-box L parameter CASE-C

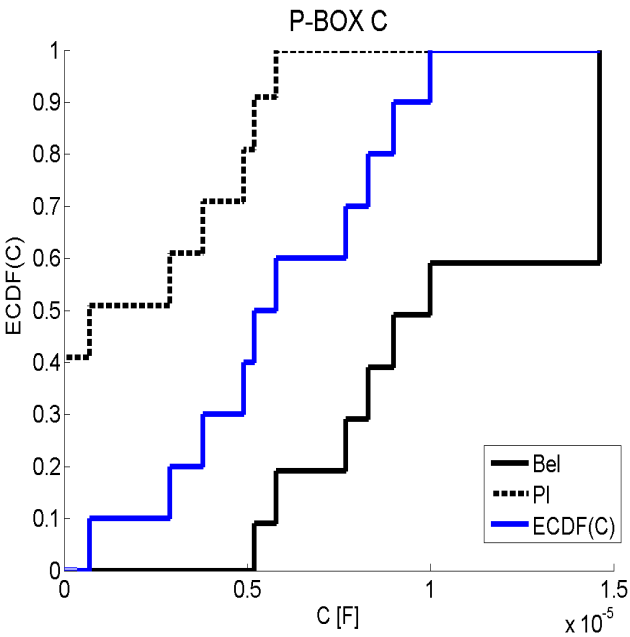


Figure 13: P-box C parameter CASE-C

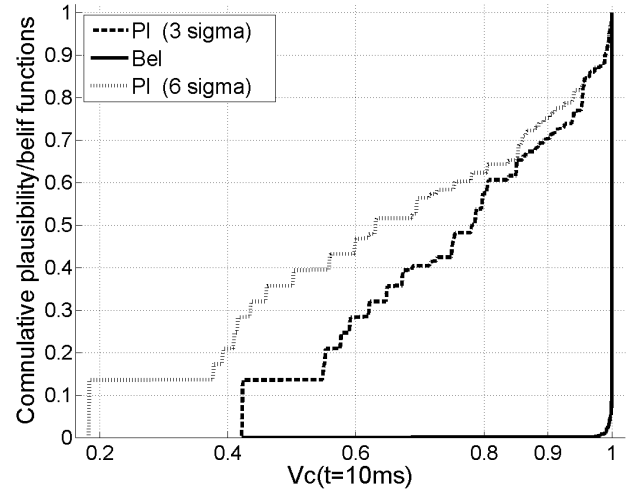


Figure 14: Qualitative variation in the probability bounds if maximum selected equal to mean plus 3 or 6 standard deviations

5.3 CASE D

In this last task, bounds of the parameters are provided, similarly to CASE-A. However, just one bound is precisely defined for each parameter. More precisely, the imprecisely defined bounds are the upper bounds of R and L and the lower bounds of C. Information for CASE-C is provided in the challenge as shown in Table 5.

The case-D, similarly to CASE-B, does not have a precise information about the parameters range. The lower bound of C could be any value between zero and 7 while the upper bound of R and L could take any value up to the infinite (even though, in practice, it is not possible). Lower bounds can be fixed by physical consideration on the parameter C, which have to be positive. The upper bounds of L and R can be better defined by e.g. some physical consideration, but to do this further information have to be assumed available. It is clear that in the real world the parameter cannot be infinite. Thus, in order to solve this case, the upper bound for the resistance RU has been considered varying within the interval, $[650, R_{Umax}]$, the upper bound of the inductance LU has been assumed varying within the interval $[6 \times 10^{-3}, L_{Umax}]$ and finally, the lower bound for the capacitance CL has been assumed lying within the interval $[C_{Lmin}, 7 \times 10^{-6}]$.

Classical Approach

Within the different bounds the parameters are modelled as random variable having uniform parent distribution, consistently with the maximum entropy Principe. Finally, all the combinations of upper and lower bounds have been analysed and failure probabilities computed via Monte Carlo simulation. In order to make this problem tractable using conventional probabilistic approaches, the bounds have been redefined as m times its nominal value for the upper

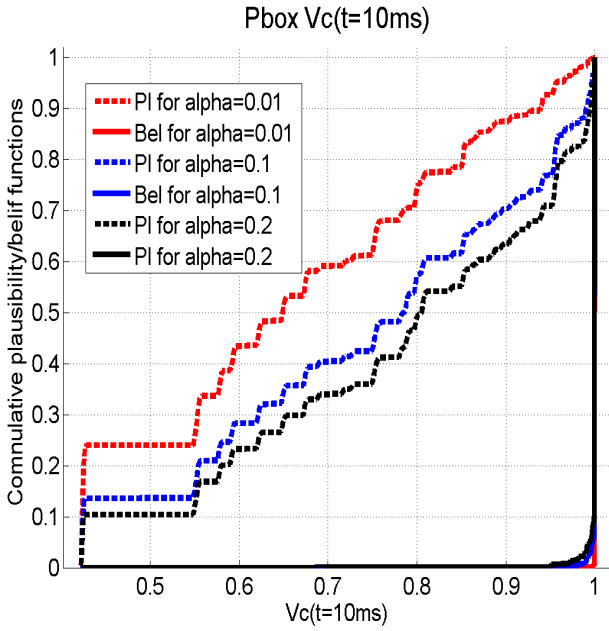


Figure 15: P-box $V_c(10ms)$, CASE-C
Pbox VC(8ms)

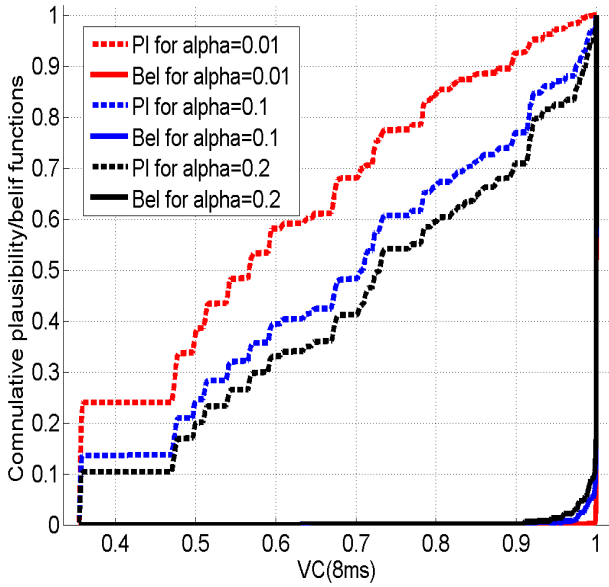


Figure 16: P-box $V_c(8ms)$, CASE-C
Pbox Z

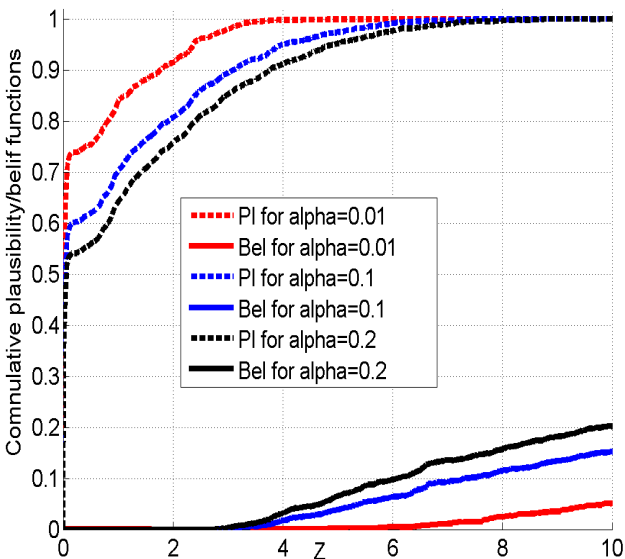


Figure 17: P-box Z, CASE-C

bounds and m divided by its nominal value for the lower bound, with $m=[1,10,100,1000]$. Having reduced the semi definite intervals to set of defined interval, it is now possible to estimate the reliability of the systems, adopting the same approach of case B.

Classical Results

It has been computed all the possible combinations of the lower and upper bounds, in order to see how the parameters interval combinations influence the results. Some combinations show probability of failure equal to 0.104. But, on the other hand, other combinations present probability of failure that is equal 1. This is due to the low efficiency of the Monte Carlo method which is not able to give a very accurate answer for small probability values. In order to accurately estimate the probability of failure in these cases, it would be necessary to estimate the probability of failure using either many more samples or by means of advanced MC methods. However, applications of advanced MC methods are out from the final purpose of this paper and have not been considered here.

Generalized Approach

The uncertainty in the parameters has been characterized by partition of the three imprecise intervals in n defined intervals, forming sets of n intervals and given by the Equations (23)-(25). Finally, same probability mass function equal to $1/n$ has been assigned to each interval (for normalization reasons) and Dempster-Shafer structures propagate similarly to previous cases.

$$\left(([R_L, \overline{R_{U1}}], \frac{1}{n}), \dots, ([R_L, \overline{R_{Umax}}], \frac{1}{n}) \right) \quad (23)$$

$$\left(([L_L, \overline{L_{U1}}], \frac{1}{n}), \dots, ([L_L, \overline{L_{Umax}}], \frac{1}{n}) \right) \quad (24)$$

$$\left(([C_{L1}, \overline{C_U}], \frac{1}{n}), \dots, ([C_{Lmin}, \overline{C_U}], \frac{1}{n}) \right) \quad (25)$$

Where i^{th} bound on the parameter (e.g. the resistance) is defined as:

$$R_{U_i} = R_{U1} + (i - 1) \frac{R_{Umax} - R_{U1}}{n}$$

Where $R_L=650\Omega$, $L_L=6mH$ and $C_U=7\mu F$. Assuming different values of L_{Umax} , R_{Umax} and C_{Lmin} may lead to different results; hence the variations in the resulting P-Boxes, due to variations the three threshold values, have been investigated. The created Dempster-Shafer structures have been propagated through the system by intervals combination similarly to the other cases. Minimum and maximum values for $V_c(8ms)$, $V_c(10ms)$ and Z are computed and stored for each interval cell. The resulting Dempster-Shafer structures are assembled and translated to Probability boxes for the Voltages and damping factors.

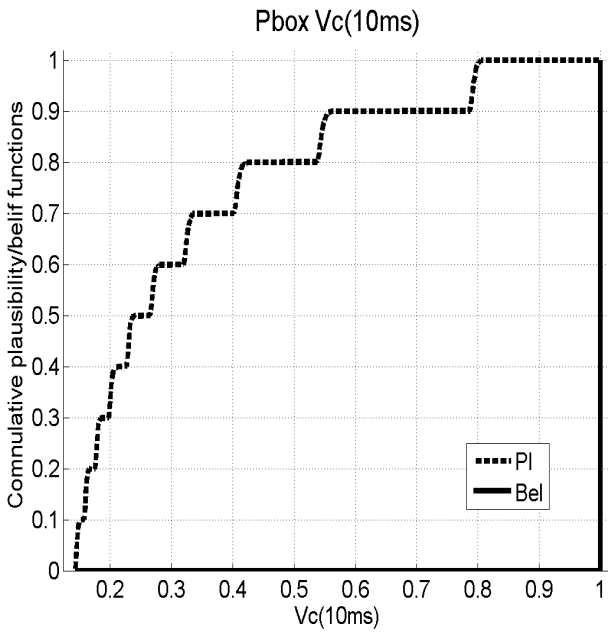


Figure 18: P-box $V_c(10ms)$, CASE-D

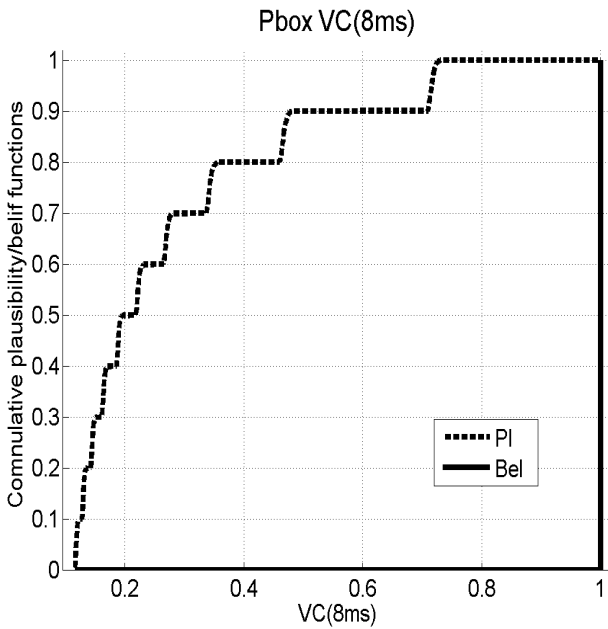


Figure 19: P-box $V_c(8ms)$, CASE-D

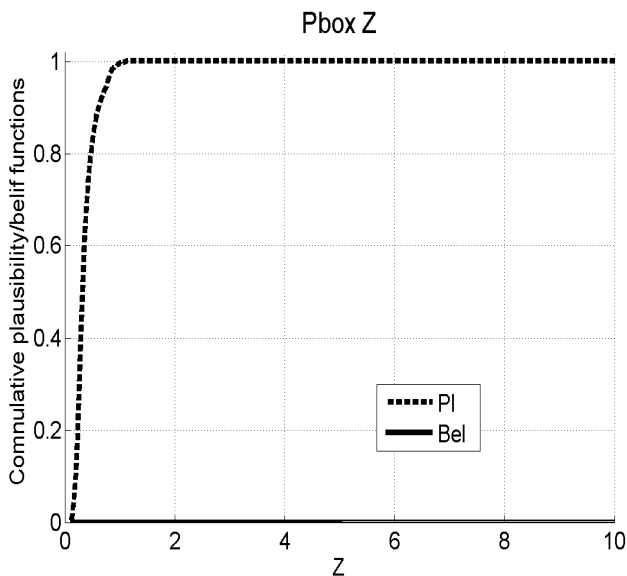


Figure 20: P-box Z , CASE-D

Generalized Results

Figures 18-20 show resulting P-Boxes for $V_c(8ms)$, $V_c(10ms)$ and Z assuming $R_{Umax}=6500\Omega$, $L_{Umax}=60mH$, $C_{Lmin}=0.7\mu F$ and $n=10$. It can be noticed that probability of failure considering for the voltage requirements lays within the interval $[0,1]$ and for the third requirements on Z lay in the interval $[0,0.99]$. Thus, the uncertainty in the inputs defined in the CASE-D is too large to provide useful results. The probability bounds for CASE-D results slightly different form the probability intervals for CASE-A (bounds equal to $[0,1]$ for all the requirements), hence the information compared to CASE B or CASE C can be seen having the highest amount of uncertainty associate and be of lower quality for the meeting requirements prospective.

Additionally, in order to investigate the effect of the assumptions on the results, the uncertainties have propagated changing the values of R_{Umax} , L_{Umax} and C_{Lmin} . Results of this analysis show that R_{Umax} is affecting more the shape of the P-Boxes. On the other hand, it has not highlighted any relevant changes in the bounds of the failure probability.

Comparing the results of probabilistic approaches and generalized approaches point out that the generalized probabilistic approaches can gave valuable prospective on the final solutions providing evidence of the low empirical quality of the available parameter data.

6 LIMITATION FACED IN APPLYING THE APPROACHES

Classical probabilistic approaches required the definition of distributions. The uniform distribution was assumed to characterize parameter uncertainty in CASE-A, CASE-B and CASE-C, since it is a typical assumption for model uncertainty if no information but bounds information is given. This assumption is often regarded as a rational hypothesis that found theoretical support in the Laplaces principle of indifference (or more in general principle of maximum entropy). In CASE-C first has been assumed a finite number of combination and a DOE, secondly it has been considered just a pdf fitted using Gaussian Kernel Density estimation. Subjectively assuming probability distribution functions can bear an underestimation of the uncertainty. As example consider the cumulative distribution function (CDF) of the uniform distribution; the CDF will have a well-known linearly increasing shape between minimum and maximum values. If these minimum and maximum bounds values are the only available data, the assumption can led to misleading results, especially in reliability assessments. Within an imprecise-information scenario (e.g. parent distribution not specified or unknown, or known but with vague parameters, conflicting and limited knowledge, linguistic incomprehension, intervals etc.), it seems more conservative and robust for the reliability assessment to take into account not just

one single CDF but all the plausible CDFs accordingly to the available data. Indeed, this approach is computationally expensive and will produce imprecise results in reliability evaluation, but has the undeniable advantage of not introducing artificial model assumption.

The analysed case study confirm that artificial model assumptions might lead to uncertainty underestimation, hence reliability results that do not represent precisely the real data's quality. Another point to be highlighted is the low efficiency of Monte Carlo method to compute small probabilities of failure. For extreme cases, where there are too few failures or too few successes, Monte Carlo is not efficient in producing accurate result. To have it more precise, it would be necessary to use another method of accuracy, e.g. Line Sampling. In the proposed study a simple system has been analysed, therefore computations were not time expensive. Drawback of the generalized approach is that high computational effort may be required, especially for the analysis of more complex systems.

Nevertheless, results obtained by generalized approaches provide valuable evidence about the quality of the information available in all the tasks which, in this case, result fairly low. The large epistemic uncertainty and lack of knowledge about the system parameters may suggest to consider an investment on collecting more valuable empirical data rather than refine the model for the reliability assessment. Overall outcomes of the study highlighted some of the positive and negative aspects of embed generalized approach to classical uncertainty quantification methodologies.

7 CONCLUSIONS AND DISCUSSIONS

In this paper, the NAFEMS uncertainty quantification challenge problem has been tackled by use of classical and generalized uncertainty quantification approaches implemented in a common computational framework. Dempster-Shafer structures, P-Boxes and Kolmogorov-Smirnov tests are the tools used to tackle the problem within the generalized approach. Results have been carried out using both the approaches and comparison and discussion provided. Classical probabilistic methods provide results characterized by precise estimation of the failure probabilities. Such precise estimations are based on strong assumptions required to characterise the uncertainties. By applying generalized probabilistic methods, only bounds of the failure probability can be obtained giving a lower precision in the prediction of the system performance but on the concession for less restrictive assumptions in the uncertainty characterization. Generalised probabilistic methods propagate the imprecise in the input into imprecision on the estimation, giving a clear indicator on the quality of the analysis. On the other hands, classical probabilistic approaches are hiding such information providing a false sense of accuracy.

In fact, the results obtained using classical proba-

bilistic approaches are, as expected, included in the bounds obtained by generalized approaches. On the other hand, the values are not close to the upper bounds of the failure probability obtained by use of generalized approach. Hence it can be stated that, in the analysed case, the less reliable or worst case scenario reveals to be underestimated by classical approach. Possible explanations are the strong initial assumptions used to define the underlying distribution for the parameters (e.g. using uniform distribution). The results seem confirming that Dempster-Shafer approach produces bounds that get narrower with better empirical information. Moreover, Dempster-Shaffer approach seems particularly useful especially in reliability assessments where probabilistic characterizations are desired and empirical information is limited. In conclusion, some of the limitation and shortcoming of the approaches have been highlighted, strength of combine classical and generalized approaches have been outlined and the computational tool verified to be flexible and effective. Generalized methods, although computational expensive, are generally applicable and they are able to provide essential information about the quality of the analysis, an unavoidable tool for the industry which may rely on more accurate information qualification approaches, understanding if the data is of high quality or poor quality aiming at designing safer and more reliable systems or components.

REFERENCES

- Alex Diaz De La O, Edoardo Patelli, M. B. I. S. A. (2014). Uncertainty quantification and management through bayesian and/or imprecise probability perspective. In *CST2014 The Twelfth International Conference on Computational Structures Technology CST2014-S08*.
- Augustin, T. (2004). Optimal decisions under complex uncertainty - basic notions and a general algorithm for data-based decision making with partial prior knowledge described by interval probability. *Special Issue of ZAMM - Zeitschrift für Angewandte Mathematik und Mechanik* 84(10–11), 1–10.
- Beer, M., S. Ferson, & V. Kreinovich (2013). Imprecise probabilities in engineering analyses. *Mechanical Systems and Signal Processing* 37(1-2), 4–29.
- Blair, A. N., B. M. Ayyub, & W. J. Bender (2001). Fuzzy stochastic risk-based decision analysis with the mobile offshore base as a case study. *Marine Structures* 14(12), 69 – 88. Very Large Floating Structures (VLFS) Part {II}.
- Ching, J. & Y.-C. Chen (2007). Transitional markov chain monte carlo method for bayesian model updating, model class selection, and model averaging. *Journal of engineering mechanics* 133(7), 816–832.
- Der Kiureghian, A. & O. Ditlevsen (2009). Aleatory or epistemic? does it matter? *Structural Safety* 31(2), 105–112.
- Dubois, D. & H. Prade (1988). *Possibility Theory*. New York: Plenum Press.
- Faber, M. H. (2005). On the treatment of uncertainties and probabilities in engineering decision analysis. *Journal of Offshore Mechanics and Arctic Engineering* 127, 243–248.
- Ferson, S., V. Kreinovich, L. Ginzburg, D. S. Myers, & K. Sentz (2002). *Constructing probability boxes and Dempster-Shafer structures*, Volume 835. Sandia National Laboratories.
- Helton, J., J. Johnson, & W. Oberkampf (2004). An explo-

- ration of alternative approaches to the representation of uncertainty in model predictions. *Reliability Engineering & System Safety* 85(13), 39 – 71. Alternative Representations of Epistemic Uncertainty.
- Kiureghian, A. D. (2008). Analysis of structural reliability under parameter uncertainties. *Probabilistic Engineering Mechanics* 23(4), 351–358.
- Laura P. Swiler, Thomas L. Paez, R. L. M. (2009). Epistemic uncertainty quantification tutorial. *Proceedings of the IMAC-XXVII*.
- Marseguerra, M. & E. Zio (2002). *Basics of the Monte Carlo Method with Application to System Reliability*. Hagen, Germany: LiLoLe - Verlag GmbH (Publ. Co. Ltd.). ISBN 3-934447-06-6.
- Massey, F. (1951). The kolmogorov-smirnov test for goodness of fit. *Journal of the American Statistical Association* 46(253), 6878.
- NAFEMS (2013, June). Challenge problem retrieved from. World Congress Salzburg, Austria.
- NAFEMS (2014). Bench mark challenge in uncertainty quantification. *THE INTERNATIONAL MAGAZINE FOR ENGINEERING DESIGNERS & ANALYSTS FROM NAFEMS*, 40–43.
- Patelli, E., D. A. Alvarez, M. Broggi, & M. de Angelis (2014). An integrated and efficient numerical framework for uncertainty quantification: application to the nasa langley multi-disciplinary uncertainty quantification challenge. *16th AIAA Non-Deterministic Approaches Conference (SciTech 2014)*, 2014–1501.
- Patelli, E., M. Broggi, M. Angelis, & M. Beer (2014, June). Opencossan: An efficient open tool for dealing with epistemic and aleatory uncertainties. In *Vulnerability, Uncertainty, and Risk*, pp. 2564–2573–. American Society of Civil Engineers.
- Pedroni, N., E. Zio, E. Ferrario, A. Pasanisi, & M. Couplet (2013). Hierarchical propagation of probabilistic and non-probabilistic uncertainty in the parameters of a risk model. *Computers & Structures* 126(0), 199 – 213. Uncertainty Quantification in structural analysis and design: To commemorate Professor Gerhart I. Schueller for his life-time contribution in the area of computational stochastic mechanics.
- Pradlwarter, H. & G. Schuller (2008). The use of kernel densities and confidence intervals to cope with insufficient data in validation experiments. *Computer Methods in Applied Mechanics and Engineering* 197(2932), 2550 – 2560. Validation Challenge Workshop.
- Rocchetta, R., Y. Li, & E. Zio (2015). Risk assessment and risk-cost optimization of distributed power generation systems considering extreme weather conditions. *Reliability Engineering & System Safety* 136(0), 47 – 61.
- Shafer, G. (1976). *A Mathematical Theory of Evidence*. Princeton: Princeton University Press.
- Silverman, B. W. (1986). *Density estimation for statistics and data analysis*, Volume 26. CRC press.
- Veneziano, D., A. Agarwal, & E. Karaca (2009). Decision making with epistemic uncertainty under safety constraints: An application to seismic design. *Probabilistic Engineering Mechanics* 24(3), 426 – 437.
- Zio, E. & N. Pedroni (2013). *Literature review of methods for representing uncertainty*, Volume 3. Foundation for an Industrial Safety Culture, Toulouse, France.

ON BAYESIAN APPROACHES FOR REAL-TIME CRACK DETECTION

R. Rocchetta & M. Broggi & E. Patelli & Quentin Huchet

Institute of Risk and Uncertainty, University of Liverpool, United Kingdom Tel.: 0044 (0) 151 7944079

ABSTRACT: Fatigue is the most dangerous failure mode for mechanical components subject to alternating loads. Due to repeated loading and unloading, one or several cracks can be initiated and propagated through the cross section of the structure. Once a critical crack length is exceeded, the structure will catastrophically fail even for stress level much lower than the design stress limit. Non-destructive inspections may be performed at predetermined time intervals in order to detect the cracks. Alternatively, a continuous monitoring of the dynamic response of the structure can allow real-time cracks detection and corrective maintenance procedures might be taken in case the monitoring procedure identifies a crack.

In this paper, Bayesian model updating procedures is adopted for the detection of crack location and length on a suspension arm, normally used by automotive industry. Experimental data of the damaged structure (frequency response function) are simulated using a high-fidelity numerical model of the arm. A second, coarse-model represents the model to be updated where cracks of random locations and dimensions are introduced. The idea underlining the approach is to identify the most probable model consistent with the observations.

The likelihood is the key mathematical formulation to include the experimental knowledge in the updating of the probabilistic model. Different likelihood functions can be used based on different mathematical assumptions. In this work, the effect of different likelihood functions will be compared to verify the capability of Bayesian procedure for system health monitoring. The different likelihoods will be categorized according to the accuracy of the results and the efficiency of the numerical procedure.

1 INTRODUCTION

Failure for mechanical components subject to alternating loads may occur in several different ways, and failures due to fatigue are one of the most dangerous types. It is well known that cyclic loads can initiate cracks which propagate through the cross section of the structures. Once a critical crack length is exceeded, the structure will catastrophically and suddenly fail, even for stress level much lower than the design stress (Paris and Erdogan 1963). In particular, interactions may occur between the structural responses and cracks in components subject to high frequency dynamic excitations, leading to vibration-induced fatigue. Consequences may be a premature failure of the component or even worst the loss of the structures which rely on the component integrity.

Several strategies are accountable to prevent sudden failures; for instance, non-destructive inspections may be performed at predetermined time intervals, in order to detect the cracks (Faber et al. 1996); however failure can occur between inspections

(Beaurepaire et al. 2012). Alternatively, a continuous monitoring of the dynamic response of the structure can allow for real-time crack detection and for a timely intervention with maintenance procedures (Chang et al. 2003). Repair actions are taken in case the monitoring procedure successfully identifies a crack which jeopardizes the structure.

In both cases, the procedure may fail in identifying a crack, leading to fatigue failure. Thus, an efficient crack detection procedure is required in order to avoid the loss of the structure. New emerging techniques are now available in the field of computational mechanics, which can be employed to assist in the monitoring of the health of the structures. These techniques modify some specific parameters in a numerical model to ensure a good agreement with the data, a so-called inverse problem. A computational framework well fitted for the solution of such inverse problems is the model updating (Fritzen et al. 1988).

In previous work (Beaurepaire et al. 2013), some of the authors implemented an updating framework for the detection of cracks in a suspension arm,

as normally used by automotive industry. The mechanical behaviour of a device was characterized by collecting Frequency Response Functions (FRF) data at a specific location.

In this paper, the updating procedure for crack detection has been further investigated and extended, aiming at better understand its limitations and strengths. Different empirical likelihood expressions have been proposed in order to fit the procedure with different features of experimental evidence. The empirical formulation are compared and discussed in two representative cases; first, the detection of a single crack of known position and not-known length, secondly, the detection of a single crack of not-known position and not-known length.

Computational time is a an issue for real-time application of the procedure and it has been addressed. As a matter of fact, many model evaluations are required for the approach, thus a strategy for the parallelization of the simulations is provided. Moreover, adopting surrogate models such as Artificial Neural Networks (ANN) and Poly-harmonic spline (PHS) the computational time has been further reduced. The general purpose software OpenCossan (Patelli et al. 2014) has been employed in all the stages of the procedure.

The paper is structured as follows: Section 2 deals with the modelling of fracture in a Finite Element framework. Section 3 outlines the main concept of Bayesian model updating and the efficient simulation algorithm employed in the particular case of structure with cracks under dynamic excitation. A numerical example and results are presented and discussed in Section 4, and likelihood expressions are compared for the two considered cases. Finally, conclusions and remarks are drawn in Section 7

2 MODELLING AND RELATED BACKGROUND

Finite element (FE) analysis has become established as a powerful family of methods for the spatial approximation of systems of partial differential equations and variational problems. It has been used in a multitude of areas in the engineering field, e.g. in the analysis of mechanical components or structures. Nevertheless, the mechanical behaviour of structures may be altered if the elements are crossed by cracks. The cross section of the component is reduced, which causes a reduction of the stiffness. Moreover, the stress field is also modified in the vicinity of a crack.

Specific FE methods have been conceived to modelling efficiently the mechanical behaviour of structures containing cracks. The extended finite elements method (XFEM), first introduced by (Moës

et al. 1999), has received considerable attention over the past few years. It consists of enriching the elements affected by a crack by introducing additional shape functions, which increases the number of degrees of freedom associated with the nodes. The stress field in these elements is then expressed using a combination of the standard and of the enrichment shape functions.

In case an element is crossed by a crack, a Heaviside function centred on the crack is introduced as an additional shape function. This step function accounts for the discontinuity of the displacements between the two lips of the crack. In case an element includes the crack tip, the corresponding nodes of the finite element model are enriched with specific shape functions. These functions correspond to the asymptotic displacement field at the vicinity of a crack tip, which can be determined analytically. For more details about the enrichment of the tip elements see (Moës et al. 1999). This allows capturing efficiently the displacement and strain fields near the crack tip, without excessive refinement of the mesh.

Details on the XFEM as implemented in the analysis here presented may be found in the works Zi and Belytschko 2003 and Abdelaziz and Hamouine 2008. However, mesh refinement in the vicinity of the crack tip may be necessary when the extended finite elements method is used, in spite of the enrichment of the nodes at the crack tip (Geniaut 2011). Nevertheless, the mesh does not have to be compatible with the crack, which considerably simplifies the re-meshing.

In case the behaviour of a cracked structure under dynamic excitation needs to be determined, the stiffness matrix may be computed using the XFEM, as stated above. The mass matrix is not modified by the presence of cracks, and no special action needs to be taken. The problem is subsequently solved using the standard procedure for linear dynamics: the modes and frequency of vibration are determined by solving the eigen-value problem associated with the mass and stiffness matrices; and the FRF associated with any node of the finite element model are determined.

3 MODEL UPDATING PROCEDURE FOR CRACK DETECTION

3.1 Bayesian updating of structural models

A Bayesian model updating procedure is based on the very well-known Bayes theorem (Bayes 1763). The general formulation is the following:

$$P(\boldsymbol{\theta}|D, I) = \frac{P(D|\boldsymbol{\theta}, I) P(\boldsymbol{\theta}|I)}{P(D|I)} \quad (1)$$

where θ represents any hypothesis to be tested, e.g., the value of the model parameters, D is the available data or observations, and I is the background information. Main terms can be identified in the Bayes theorem:

- $P(D|\theta, I)$ is the likelihood function of the data D ;
- $P(\theta|I)$ is the prior probability density function (PDF) of the parameters;
- $P(\theta|D, I)$ is the posterior PDF;
- $P(D|I)$ is a normalization factor ensuring that the posterior PDF integrates to 1;

The theorem introduces a way to update some a-priori knowledge on the parameters θ , by using data or observations D and conditional to some available information or hypothesis I .

Bayes law has been successfully applied in the updating of structural models see (Beck and Katafygiotis 1998) and (Katafygiotis and Beck 1998); in particular the Bayesian structural model updating has been successfully used to update large finite element models using experimental modal data (Goller et al. 2011). In a structural model updating framework, the initial knowledge about the unknown adjustable parameters, e.g. from prior expertise, is expressed through the prior PDF. A proper prior distribution can be a uniform distribution in the case when only a lower and upper bound of the parameter is known, or a Gaussian distribution when the mean and a relative error of the parameter is known.

The likelihood function gives a measure of the agreement between the available experimental data and the corresponding numerical model output. Particular care has to be taken in the definition of the likelihood, and the choice of likelihood depends on the type of data available, e.g. whether the data is a scalar or a vector quantity. Different likelihood leads to different accuracy and efficiency in the results of the updating procedure and should be selected with caution; as an example, the use of unsuitable likelihood function might cause that the model updating do not produce any relevant variation in the prior.

Finally, the posterior distribution expresses the updated knowledge about the parameters, providing information on which parameter ranges are more probable based on the initial knowledge and the experimental data.

3.2 Transitional Markov-Chain Monte-Carlo

The Bayesian updating expressed in equation 1 needs a normalizing factor, that can be very complex to

obtain and computationally expensive. An effective stochastic simulation algorithm, called Transitional Markov Chain Monte-Carlo (Ching and Chen 2007), has been used in this analysis. This algorithm allows the generation of samples from the complex shaped unknown posterior distribution through an iterative approach. In this algorithm, m intermediate distributions P_i are introduced:

$$P_i \propto P(D|\theta, I)^{\beta_i} P(\theta|I) \quad (2)$$

where the contribution of the likelihood is scaled down by an exponent β_i , with $0 = \beta_0 < \dots < \beta_i < \dots < \beta_m = 1$, thus the first distribution is the prior PDF, and the last is the posterior. The value of these exponents β_i is automatically selected to ensure that the dispersion of the samples at each step meet a prescribed target. For additional information the reader is reminded to (Ching and Chen 2007). These intermediate distributions show a more gradual change in the shape from one step to the next when compared with the shape variation from the prior to the posterior.

In the first step, samples are generated from the prior PDF using direct Monte-Carlo. Then, sample from the P_{i+1} distribution are generated using Markov chains with the Metropolis-Hasting algorithm (Hastings 1970), starting from selected samples taken from the P_i distribution, and β_i is updated. This step is repeated until the distribution characterized by $\beta_i = 1$ is reached. By using the Metropolis-Hasting algorithm, samples are generated from the posterior PDF without the necessity of ever computing the normalization constant. By employing intermediate distributions, it is easier for the updating procedure to generate samples also from posterior showing very complex distribution, e.g., very peaked around a mean value or showing a multi-modal behaviour.

3.3 Model updating for crack detection and likelihood expression

In the FE model, the cracks are modelled using XFEM. Experimental data from the reference structure are taken into account in the form of Frequency Response Functions. Knowing that cracks will develop most probably in certain locations, characterized by high concentration of stresses, cracks are inserted in these specific positions assuming their lengths are random parameters.

Within the model updating framework, the cracks present in the damaged structure are seen as uncertain model properties. The prior will use uniform distribution for the crack parameters, allowing the possibility of crack in any stress concentration point and with any possible physically acceptable length, i.e. compatible with geometric constraints and

material proprieties.

The likelihood is the key mathematical component of any Bayesian updating procedure. Within the proposed crack detection framework, synthetic experimental FRFs are compared with the numerical FRF of the numerical model. Within the case study, three empirical likelihood formulations are proposed and used to compare the experimental data with the numerical information. Expressions are discussed on the basis of the accuracy of the results, i.e. the ability in detecting true cracks positions and lengths.

The likelihoods have been expressed as:

$$P(D|\boldsymbol{\theta}, I) = \prod_{k=1}^{N_e} P(x_k^e; \boldsymbol{\theta}) \quad (3)$$

or, equivalently, in the form of the log-likelihood:

$$P(D|\boldsymbol{\theta}, I) = \sum_{k=1}^{N_e} \log(P(x_k^e; \boldsymbol{\theta})) \quad (4)$$

where x_k^e represent the k^{th} experimental evidence, N_e is the number of available experimental data and $\boldsymbol{\theta}$ is the vector of random crack lengths. The term $P(x_k^e; \boldsymbol{\theta})$ which include the experimental evidence have been assumed as exponentially distributed.

Three heuristic formulations have been defined as follows:

$$P(x_k^e; \boldsymbol{\theta}) \propto \exp\left(\frac{\delta_k}{MSE_{pks}[h(\boldsymbol{\theta}) - h_e^k]}\right) \quad (5)$$

$$P(x_k^e; \boldsymbol{\theta}) \propto \exp\left(\frac{\delta_k}{MSE_{low}[h(\boldsymbol{\theta}) - h_e^k]}\right) \quad (6)$$

$$P(x_k^e; \boldsymbol{\theta}) \propto \exp\left(\frac{\delta_k}{MSE_{all}[h(\boldsymbol{\theta}) - h_e^k]}\right) \quad (7)$$

where h_e^k is the experimental FRF k, $h(\boldsymbol{\theta})$ represents the numerical FRF, δ_k is the variance of the Means Square Errors (MSE) for the experiment k. The Means Square Errors have been obtained considering different frequency ranges, e.g. MSE_{all} is computed between experimental FRF and numerical FRF over the entire frequency domain, MSE_{low} is computed considering lower frequencies and MSE_{pks} is obtained around the main resonance peaks. The proposed expressions and the selection of the frequency ranges were defined on empirical basis therefore details will be discussed in the case study, Section 4.

After the updating procedure, the posterior distributions provide a qualitative indication of the crack length and positions, i.e. it will concentrate around the unknown length and position of the crack with most similar response if compared to the experimental observations.

It worth remark that even if the procedure in generally applicable to detect cracks, the component analysed have a specific FRF, which therefore limit the consideration on the validity of the defined likelihoods to the specific mechanical device in exam.

4 NUMERICAL EXAMPLES

This numerical example is similar to those used in the automotive industry (Mrzyglod and Zielinski 2006) and it has been recently applied (Beaurepaire et al. 2013) to detect cracks in a suspension arm, shown in Figure 1. It can freely rotate along the axis indicated by the dashed line; the suspension spring and the wheel structure are connected at the location indicated by "S". The stress concentration points, and candidate crack locations, are indicated in the figure by the numbers 1 to 6.

In this case study, "simulated" experimental data are generated using a Finite Element (FE) model. The software used to construct the model and in the analysis is Code Aster (Geniaut 2011). A crack with fixed length is inserted in one of the candidate position, and the reference FRF is computed at the position indicated by "O". Both the FRF in direction X and Y are considered, while no FRF is obtained in the direction Z since the structure is not constrained in that direction. Figure 2 display the FRFs in the directions X and Y when a 5 mm length crack is considered. Just three out of six possible position are shown for graphical reasons.

The crack lengths are considered as uncertain parameters, and are modelled using uniformly distributed random variables. Since the crack is phys-

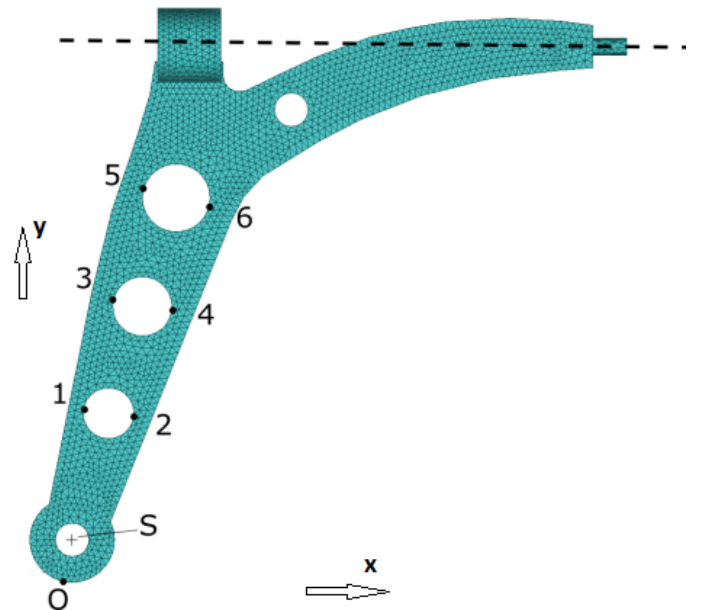


Figure 1: The suspension arm FE model with indicated the six possible crack positions and the FRF measurement point.

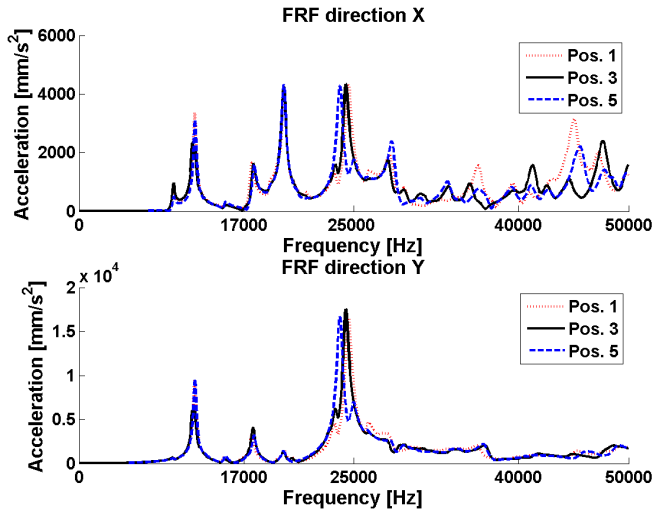


Figure 2: Frequency response functions of the high fidelity FE model. A single crack of 5mm length is inserted in each of the stress concentration points.

ically constrained to not touch the flanges of the arm, a maximum crack length of 5 mm is assigned to the cracks in position 1 and 2, while the length is limited to 10 mm for the cracks in positions 3 to 6. The sampled values of the random variables are inserted into the FE model by using the ASCII file injection routine provided by OpenCossan (Patelli et al. 2014), providing a deterministic FRF. Additionally, the simulations run in parallel on a computer cluster and surrogate model are used, allowing further reduction of the overall computational time.

The goodness of the procedure in detecting cracks has been tested for two updating cases:

- detection of single crack having known position and unknown length
- detection of a single crack of unknown position and length.

In both the cases analysis have been carried out by using empirical likelihood expressions. Results compared and discussed point out positive and negative features of the different formulations.

The likelihoods expressions and frequency ranges have been selected after considerations on the computational inaccuracy affecting numerical FRFs, especially in the high frequencies domain. It can be argued that likelihoods defined as in Equations 5 - 6 might detect cracks with higher precision if compared to Equation 7 which computes MSE including FRF values in the high frequency range. MSE_{low} in Equation 6 has been computed over the low frequency range from 0 Hz to 1.7×10^4 Hz while MSE_{all} is computed over the entire domain (from 0 Hz to 5×10^4 Hz). Furthermore, it has been noticed that the FRFs around the main resonance peaks (e.g. around 2.4×10^4 Hz in Fig. 2) appear to be particularly variable with respect to the crack positions and

lengths. Hence, MSE_{pks} has been computed around the main resonance peaks (2.4×10^4 Hz) to verify if it is a good indicator to distinguish different crack lengths and locations.

4.1 Surrogate model calibration and selection

The Bayesian model updating procedure is computationally expensive, thus surrogate models have been adopted to reduce the computational time. Among the different surrogate models, Artificial Neural Networks (ANN) and Poly-harmonic Spline (PHS) have been tested and the best model has been selected.

The classical architecture type for Artificial Neural Network (Chojaczyk et al. 2015) consists of one input layer, one or more hidden layers and one output layer. Each layer employs several neurons and each neuron in a layer is connected to the neurons in the adjacent layer with different weights. Poly-harmonic Spline is popular tool for model interpolation and has been considered as alternative surrogate model to be compared with the ANN due to their good proprieties, see e.g. in (Madych and Nelson 1990).

The coefficient of determination R^2 is often used to evaluate the quality of the regression model and have been adopted to choose the most suitable meta-model to use in the procedure. This coefficient can be expressed as follows:

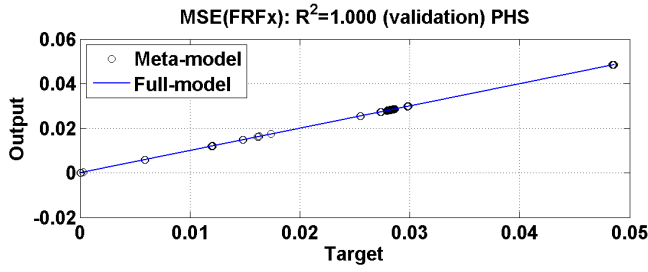
$$R^2 = 1 - \frac{\sum_i (y_i - \hat{y}_i)^2}{\sum_i (y_i - \bar{y})^2} \quad (8)$$

where y_i is the i^{th} mean square error, \hat{y}_i is the mean square error predicted by the surrogate model, \bar{y} is the average of the mean square errors from the FE analysis.

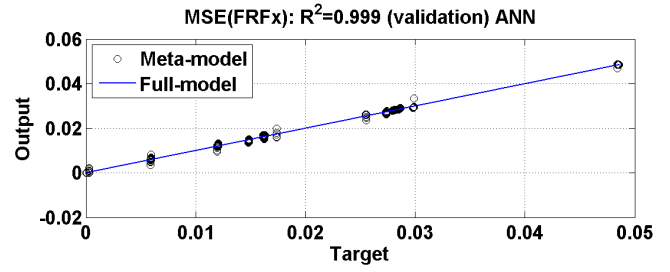
It goes without saying that R^2 values have to be fairly compared between the two considered surrogates, therefore the coefficient have to be compared on the validation set. Otherwise the R^2 for the PHS, computed using the calibration set, will result by definition equal to 1.

Input data for the surrogate models is the vector θ of simulated cracks, outputs are MSE between the simulated FRFs and a preselected synthetic experimental FRF. Both direction X and Y are considered, hence MSE in X and Y directions are the outputs of the surrogate models. In order to reduce complexity and limit the number of outputs, the entire FRF has not been considered as output for the surrogates model.

The proposed ANN layout consists of hidden layer with 11 nodes for the first two layers and 13 for the last layer. The described architecture have been

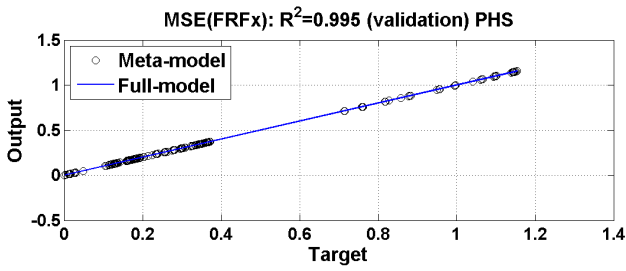


(a) PHS

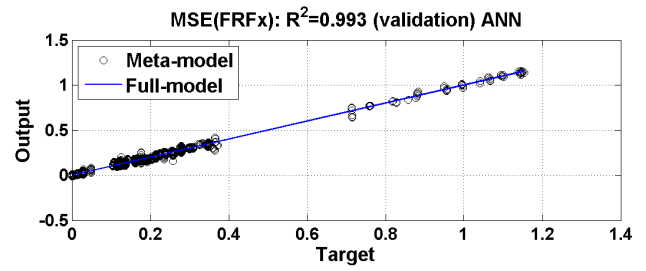


(b) ANN

Figure 3: Regression plots of meta-models for a single crack with fixed known position.



(a) PHS



(b) ANN

Figure 4: Regression plots of meta-models for a single crack of unknown position and length.

selected based on precedent results and in order to capture the highly non-linear behaviours of the outputs. Cubic PHS has been considered for model the behaviour of the MSE in x and y directions. The models have both been calibrated using 90% of the data set and validated using the remaining 10%. Examples of results are proposed in Figures 3-4 where mean square errors between experimental and simulated FRFs in X direction are considered. The targets, in the X -axis, are MSE obtained using the FE model and the outputs, in the Y -axis, represent the output of the meta-model. The sub-plots in the top of the figures display results for the model calibration, while in the bottom are displayed results for the validation set. Experimental cracks is considered in position 6 of length 8.07 mm.

In the first case 700 single crack lengths with known position (crack in position 6 in Fig. 1) have been considered. Figures 3a-3b present linear regression results for the first analysed case. Similarly, Fig-

ures 4a-4b shows linear regression plots and comparisons for the second analysed case. In the second case, 2800 single cracks of random length with not-known position are the input for the surrogate model. The R^2 values for the validation data show that PHS is the best candidate surrogate model for both the considered detection cases. Hence, PHS appear to be more suitable than ANN to mimic the MSE behaviour. This can be explained if considered the “step” behaviour of the outputs along the crack length. In order to reproduce this non-linear behaviour, an ANN need to be built with several nodes and several hidden layers; on the other hand, a PHS works well in capturing it because it is obliged to pass through the support points and better predict non-linearly in-between the supports.

4.1.1 Single crack, known position

Bayesian updating procedure has been used first to detect of single crack length which has a known position (position 6 in Fig. 1). The procedure starts

by first selecting prior distribution for the crack length $P(\theta|I) \sim U[0, 10]$ and sample number equal to 1500. Number of samples has been selected based on previous works, however future optimization of the initial setting might be considered to reduce the computational time. Three different synthetic experimental FRFs have been selected, corresponding to cracks of “short” length (2.4 mm) “medium” length (4.53 mm) and “long” length (8.07 mm). Updating procedure has been repeated to include the empirical likelihoods defined in Section 3.3. Results have been qualitatively ranked based on the accuracy of the posterior distributions; suitability of the likelihoods is discussed.

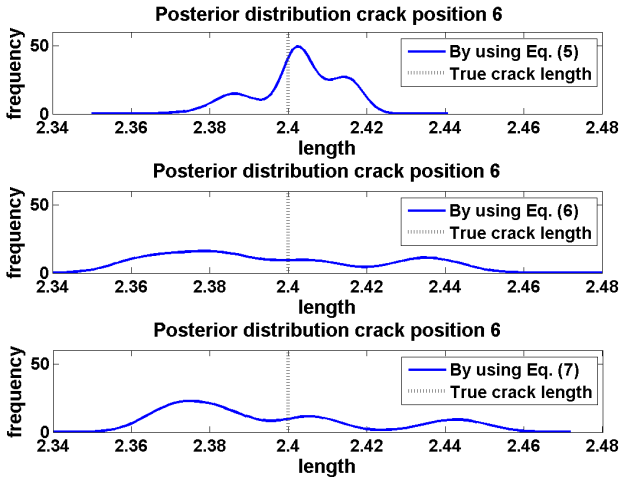


Figure 5: Posterior distribution of “short” crack length in position 6, different likelihoods expressions.

In Figure 5 shows posterior distributions for different likelihoods and for a crack lengths to be detected equal to 2.4 mm. The posterior distributions result peaked around the true crack length. The crack length is detected with high precision in this case; mean values for the distribution are almost equal to the true crack lengths 2.4 mm plotted in dotted line. Among the three analysed likelihoods, the one computed using Equation 5 result in a lower variance compared to the others, as can be qualitatively observed in the top sub-plot of Figure 5. Similar behaviour is observable for the other selected crack lengths.

Nevertheless, considered the final aim of the updating, the differences are of minor relevance. More specifically, in this stage of comparison which is intended to be mainly qualitative, detecting a crack with uncertainty ± 0.06 mm or ± 0.04 mm has been considered a minor difference. The crack length is detected with high precision in case of single crack with known position, and all the likelihood expressions seems well-suited to be used within the detection framework.

4.1.2 Single crack, unknown position

The procedure presented in 4.1.1 has been extended for detect both the length and position of a crack. The procedure, has been tested considering likelihoods described in Section 3.3, and assuming uniform prior distributions for cracks in position 3 to 6 ($P(\theta|I) \sim U[0, 10]$) and in position 1 and 2 ($P(\theta|I) \sim U[0, 5]$). The synthetic experimental FRF is the one of a crack in position six of length 8.07 mm.

Figures 6, 7 and 8 display the posterior distributions obtained by using likelihoods computed as in equations 5, 6 and 7 respectively. Results indicate correct detection of the crack within the true length range and the true position.

Computing likelihood considering main resonance frequency, as in Figure 6 crack is detected within the length interval [7-10 mm]. Similar results, displayed in Figures 7 and 8, are obtained by using different likelihood expressions. The results show higher uncertainty if compared to the results in Section 4.1.1. The posterior distributions for cracks in positions from 1 to 5 result similar to the assumed prior uniform distributions. This mean that none of the simulated cracks length in positions form 1 to 5 can be fairly associated to the experimental evidence provided. However, results obtained by using Equation 6 wrongly detect a crack in position 4 of approximate length of 5 mm. Explanation might be found considering the FRF behaviour in the low frequencies range. The updating procedure may have revealed similarity between experimental data of “long” crack in position 6 and simulated FRF for cracks of mean length in position 4.

5 NOISE ANALYSIS AND UPDATING

In order to increase adherence to reality, noises have been added to the synthetic experimental FRF (simulated). Signal-to-noise ratio (SNR) can be defined as the ratio between the power of the signal and power of the noise affecting the signal; input SNRs lower than 20 dB are typically encountered at the resonance frequency of lightly damped vibrating mechanical structures.

The noise function has been added to the FRF as explained in equations 9-10.

$$FRF_x = FRF_x + N_x \quad (9)$$

$$FRF_y = FRF_y + N_y \quad (10)$$

Where N_x and N_y are noises in the X and Y axis directions respectively. General case of correlated noises in the X and Y directions has been considered, consistently with the fact that noises in different directions are often generated by common sources

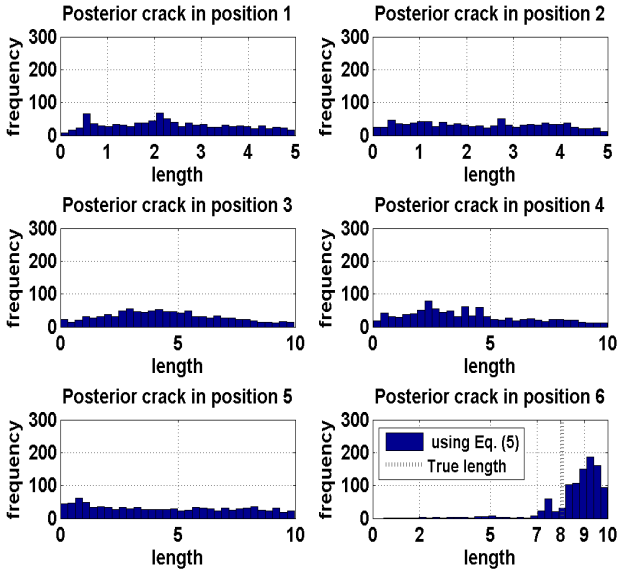


Figure 6: Likelihood computed with MSE_{pks} .

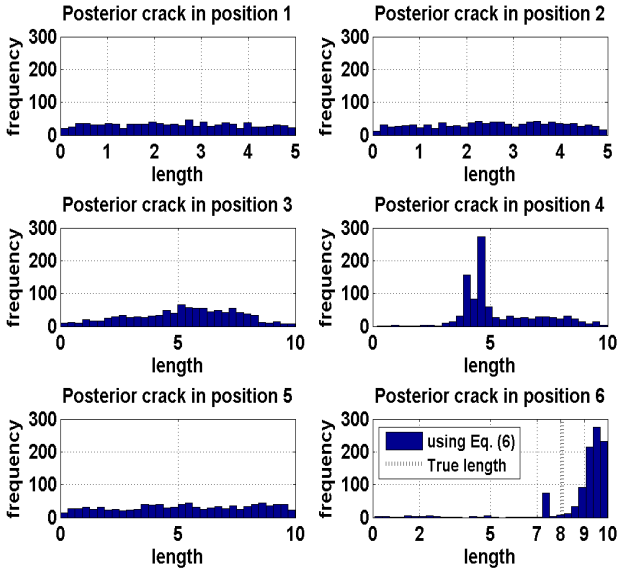


Figure 7: Likelihood computed with MSE_{low} .

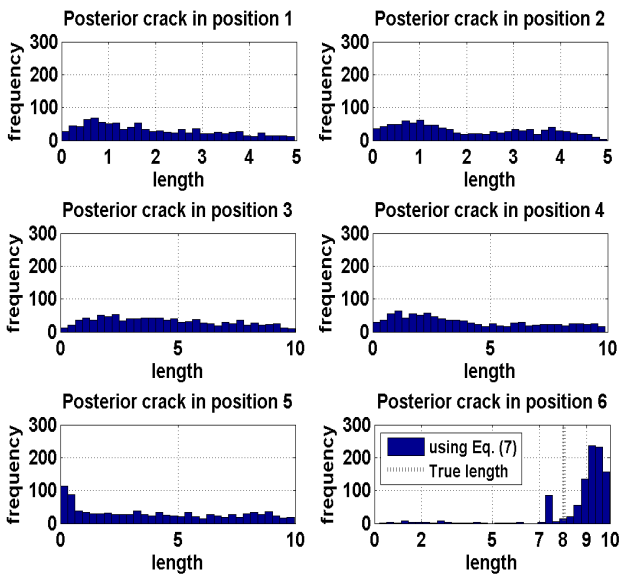


Figure 8: Likelihood computed with MSE_{all} .

(e.g. noise on the signal input, external environment, etc.). The goodness of the detection has been tested if three predefined level of SNR are added to the reference FRFs. The SNR have been set equal to 100 dB (almost negligible noise), 30 dB and 10 dB (fairly noisy). An indicative plot of FRF in x direction adding different noise levels is shown in figures 9-10.

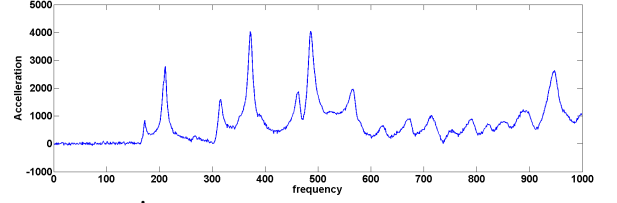


Figure 9: FRF_x with added noise equal to 30 dB SNR.

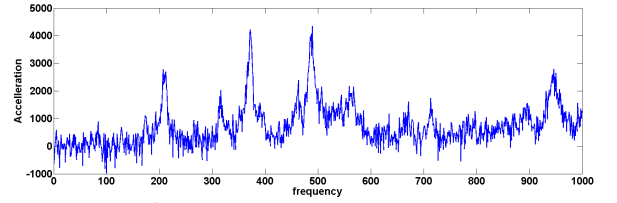


Figure 10: FRF_x with added noise equal to 10 dB SNR.

5.1 Results of Updating including noises

Figure 11 displays Kernel-Density fitted posterior distributions. The results have been obtained using three synthetic experimental crack lengths in position 6 (short, medium and long lengths) and by adding noise as previously indicated in section 6. The posterior distributions obtained for the other possible crack locations (one to five) result approximately uniform, therefore not displayed for synthesis reasons.

As expected, the accuracy in the detection deteriorates if SNR decrease (noise intensity increase). It can be observed that for SNE equal to 100 dB, posterior distribution is peaked around the true crack length, while increasing the noises to ratio to 30 dB lower and upper bounds of the pdf result less narrow. Finally, adding a fairly intense noise, SNR is set equal to 10dB, makes the updating procedure fail in identifying the crack (uniform distribution as posteriors).

6 ALEATORY UNCERTAINTY ON THE YOUNG'S MODULUS

In order to better understand the role played by aleatory uncertainty in the updating procedure intrinsic randomness has been considered in one of the suspension arm parameters. The Youngs modulus E has been considered as the aleatory parameter, assumed normally distributed around a known mean value (initial set of the model) with a standard deviation equal

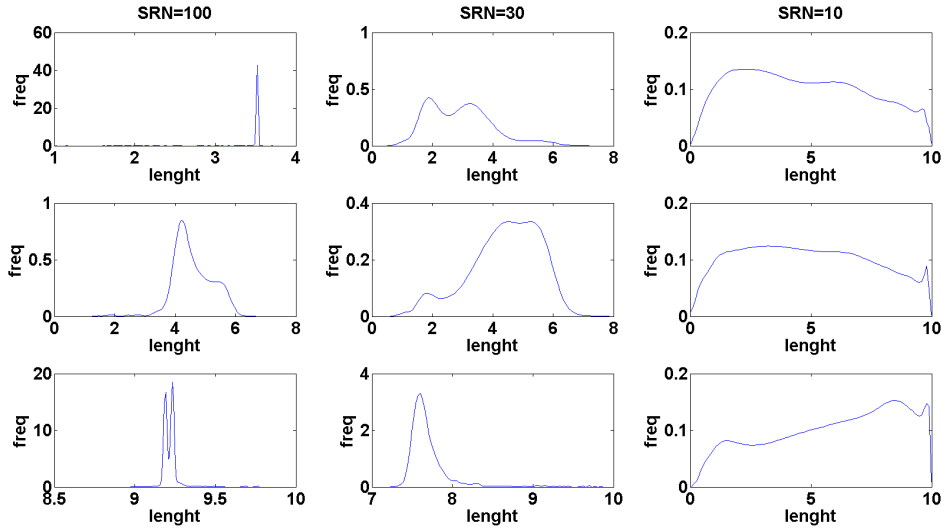


Figure 11: Posterior distribution results three noise level and three crack lengths in position 6.

to 3% of the mean value. Number 500 parallelized Monte Carlo (MC) runs, coupled with the FE solver have been performed and as many FRFs in directions X and Y stored. The suspension arm has been considered as a perfectly homogeneous with respect to E , hence each element of the FE model share the same sampled E within the single MC run. The FRF results for sampled normal random E modulus are shown in figure 12.

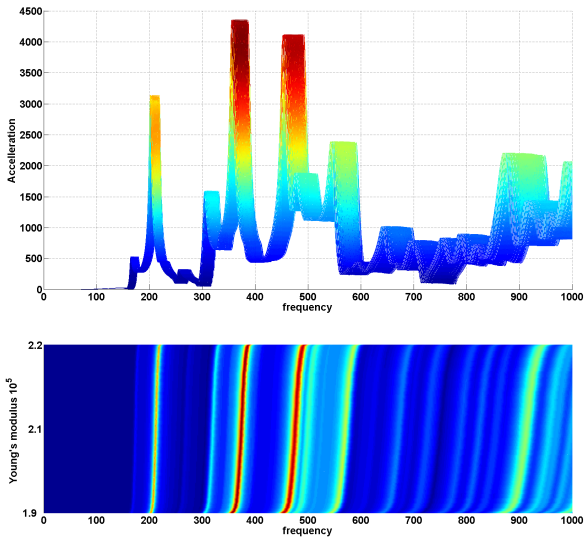


Figure 12: Variability of the frequency response function with E .

As can be noticed, there is a high variability in the FRFs profile due to uncertainty in the E modulus, even if some regularity is observable i.e. FRF shapes seem to be very similar. It is worth highlighting that the spectrum of uncertainty associated to the aleatory uncertainty in the E modulus is fairly large and together to epistemic uncertainty due to lack of knowledge about the true crack parameters makes the updating procedure more challenging. Nevertheless, particular patterns in the FRF peaks and improved comparison estimator between FRFs may be used to tune the up-

dating and improve the robustness of the detection, which can be seen as a future research direction.

7 REMARKS AND CONCLUSIONS

A Bayesian model updating procedure for cracks detection has been presented and it has been applied to detect cracks in a suspension arm. Reference dynamic data from vibration analysis was used as target for the updating. The effects of different likelihood expressions and different experimental data on the crack detection strategy have been analysed. The procedure has been tested first to detect a single crack with unknown length but known position, the result comparison did not suggest major differences between the likelihood formulas. Nevertheless, the second case points out the limitations of some of them. It is possibly due to similarity in the FRF for different cracks or shortcomings in the computational accuracy. In both the analysed cases, the crack was detected correctly around the true length and position. Aleatory uncertainty has been added to the FRF under the form of noises of different intensity. Furthermore, randomness in one of the suspension arm parameters has been accounted. Preliminary results show, as expected, reduced precision of the detection if high noises are accounted for. Moreover, uncertainty in the Young's modulus shows relatively high variability of the FRF results, which can be seen as a further issue for an effective model updating. Future development and additional research will be taken by using real experimental data to further validate and expand the proposed approach, advanced noise filtering techniques to reduce rumours and more efficient indicators for the FRF comparison are going to be considered.

REFERENCES

Abdelaziz, Y. & A. Hamouine (2008). A survey of the extended finite element. *Computers & Structures* 86(11-12), 1141–

- Bayes, T. (1763). An essay towards solving a problem in the doctrine of chances. *Philosophical Transactions of the Royal Society of London* 53, 370–418.
- Beaurepaire, P., E. Patelli, & M. Broggi (2013). A bayesian model updating procedure for dynamic health monitoring. In *COMPADYN 2013 4th ECCOMAS Thematic Conference on Computational Methods in Structural Dynamics and Earthquake Engineering*.
- Beaurepaire, P., M. Valdebenito, G. Schuëller, & H. Jensen (2012). Reliability-based optimization of maintenance scheduling of mechanical components under fatigue. *CMAME* 221-222, 24–40.
- Beck, J. L. & L. S. Katafygiotis (1998). Updating models and their uncertainties. i: Bayesian statistical framework. *Journal of Engineering Mechanics, ASCE* 124(4), 455–461.
- Chang, P., A. Flatau, & S. Liu (2003). Review paper: health monitoring of civil infrastructure. *Structural Health Monitoring* 3.
- Ching, J. & Y.-C. Chen (2007). Transitional markov chain monte carlo method for bayesian model updating, model class selection, and model averaging. *Journal of engineering mechanics* 133(7), 816–832.
- Chojaczyk, A., A. Teixeira, L. Neves, J. Cardoso, & C. G. Soares (2015). Review and application of artificial neural networks models in reliability analysis of steel structures. *Structural Safety* 52, Part A, 78 – 89.
- Faber, M., I. Kroon, & J. Srensen (1996). Sensitivities in structural maintenance planning. *Reliability Engineering & System Safety* 51(3), 317 – 329. Maintenance and reliability.
- Fritzen, C., D. Jennein, & T. Kiefer (1988). Damage detection based on model updating methods. *Mechanical Systems and Signal Processing* 12, 163 186.
- Geniaut, S. (2011). Code aster, notice d'utilisation de la methode x-fem (in french). technical report u2.05.02. Technical report, EDF-R&D.
- Goller, B., M. Broggi, A. Calvi, & G. Schuëller (2011). A stochastic model updating technique for complex aerospace structures. *Finite Elements in Analysis and Design* 47(7), 739–752.
- Hastings, W. (1970). Monte carlo sampling methods using markov chains and their applications. *Biometrika* 82, 711–732.
- Katafygiotis, L. S. & J. L. Beck (1998). Updating models and their uncertainties ii: Model identifiability. *Journal of Engineering Mechanics, ASCE* 124(4), 463–467.
- Madych, W. & S. Nelson (1990). Polyharmonic cardinal splines. *Journal of Approximation Theory* 60(2), 141 – 156.
- Moës, N., J. Dolbow, & T. Belytschko (1999). A finite element method for crack growth without remeshing. *Int. J. Numer. Meth. Engng* 46, 131–150.
- Mrzyglod, M. & A. P. Zielinski (2006). Numerical implementation of multiaxial high-cycle fatigue criterion to structural optimization. *Journal of Theoretical and Applied Mechanics* 44(3), 691–712.
- Paris, P. & F. Erdogan (1963). A critical analysis of crack propagation laws. *J. Basic Eng., Trans. ASME* 85, 528–534.
- Patelli, E., M. Broggi, M. de Angelis, & M. Beer (2014). OpenCOSSAN: an efficient open tool for dealing with epistemic and aleatory uncertainties. *Vulnerability, Uncertainty, and Risk: Analysis, Modeling, and Management*, 2564–2573.
- Zi, G. & T. Belytschko (2003). New crack-tip elements for xfem and applications to cohesive cracks. *International Journal for Numerical Methods in Engineering* 57(15), 2221–2240.